

Almost exact Mendelian randomization

Matthew J Tudball¹, George Davey Smith¹ and Qingyuan Zhao²

¹*MRC Integrative Epidemiology Unit, University of Bristol, e-mail: matt.tudball@bristol.ac.uk; KZ.Davey-Smith@bristol.ac.uk*

²*Statistical Laboratory, University of Cambridge, e-mail: qyzhao@statslab.cam.ac.uk*

Abstract: Mendelian randomization (MR) is a natural experimental design based on the random transmission of genes from parents to offspring. However, this inferential basis is typically only implicit or used as an informal justification. As parent-offspring data becomes more widely available, we advocate a different approach to MR that is exactly based on this natural randomization, thereby formalizing the analogy between MR and randomized controlled trials. We begin by developing a causal graphical model for MR which represents several biological processes and phenomena, including population structure, gamete formation, fertilization, genetic linkage, and pleiotropy. This causal graph is then used to detect biases in population-based MR studies and identify sufficient confounder adjustment sets to correct these biases. We then propose a randomization test in the within-family MR design using the exogenous randomness in meiosis and fertilization, which is extensively studied in genetics. Besides its transparency and conceptual appeals, our approach also offers some practical advantages, including robustness to misspecified phenotype models, robustness to weak instruments, and elimination of bias arising from population structure, assortative mating, dynastic effects, and horizontal pleiotropy. We conclude with an analysis of a pair of negative and positive controls in the Avon Longitudinal Study of Parents and Children. The accompanying R package can be found at <https://github.com/matt-tudball/almostexactmr>.

MSC2020 subject classifications: Primary 62D20, 62G10, 62P10.

Keywords and phrases: Causal inference, Instrumental variables, Randomization test, Graphical models, Genetics.

1. Introduction

1.1. A brief history of Mendelian randomization

Mendelian randomization (MR) is a natural experimental design that uses the random allocation of genes from parents to offspring as a foundation for causal inference (Sanderson et al., 2022). The ideas behind MR can be traced back to the intertwined beginnings of modern statistics and genetics about a century ago. In one of the earliest examples, Wright (1920) used selective inbreeding of guinea pigs to investigate the causes of colour variation and, in particular, the relative contribution of heredity and environment. In a later defence of this work, Wright (1923, p. 251) argued that his analysis of path coefficients, a precursor to modern causal graphical models, “rests on the validity of the premises, i.e., on the evidence for Mendelian heridity”, and the “universality” of Mendelian laws justifies ascribing a causal interpretation to his findings.

At around the same time, Fisher (1926) was contemplating the randomization principle in experimental design and used it to justify his analysis of variance (ANOVA) procedure, which was partly motivated by genetic problems. In fact, the term “variance” first appeared in Fisher’s groundbreaking paper that bridged Darwin’s theory of evolution and Mendel’s theory of genetic inheritance (Fisher, 1918). Fisher (1935) described randomization as the “reasoned basis” (p. 12) for inference and “the physical basis of the validity of the test” (p. 17). In a later Bateson Lecture to a genetics audience, Fisher revealed that his factorial design of experiments derives “its structure and its name from the simultaneous inheritance of Mendelian factors” (Fisher, 1951, p. 330). Indeed, Fisher

viewed randomness in meiosis as uniquely shielding geneticists from the difficulties of establishing reliably controlled comparisons, remarking that “the different genotypes possible from the same mating have been beautifully randomized by the meiotic process” (Fisher, 1951, p. 332).

While this source of randomization was originally used for eliciting genetic causes of phenotypic variation, it was later identified as a possible avenue for understanding causation among modifiable phenotypes themselves. Lower et al. (1979) used N-acetylation, a phenotype of known genetic regulation and a component of detoxification pathways for arylamine, to strengthen the inference that arylamine exposure causes bladder cancer. Katan (1986) proposed to address reverse causation in the hypothesized effect of low serum cholesterol on cancer risk via polymorphisms in the apolipoprotein E (*APOE*) gene. He argued that, if low cholesterol was indeed a risk factor for cancer, we would expect to see higher rates of cancer in individuals with the low cholesterol allele. Another pioneering application of this reasoning can be found in a proposed study of the effectiveness of bone marrow transplantation relative to chemotherapy (Gray and Wheatley, 1991), for example, in the treatment of acute myeloid leukaemia (Wheatley and Gray, 2004). Patients with a compatible donor sibling were more likely to receive transplantation than patients without. Since compatibility is a consequence of random genetic assortment, comparing survival outcomes between the two groups can be viewed as akin to an intention-to-treat analysis in a randomized controlled trial. This paper appears to be the first to use the term “Mendelian randomization”. An earlier review of this prehistory of MR can be found in Davey Smith (2007).

It would be a dozen more years before an argument for the broader applicability of MR was put forward by Davey Smith and Ebrahim (2003). At the time, a number of criticisms had been levelled against the state of observational epidemiology and its methods of inquiry (Feinstein, 1988; Taubes, 1995; Davey Smith, 2001). Several high profile results failed to be corroborated by subsequent randomized controlled trials, such as the role of beta-carotene consumption in lowering risk of cardiovascular disease, with unobserved confounding identified as the likely culprit (Davey Smith, 2001, p. 329-330). This string of failures motivated the development of a more rigorous observational design with an explicit source of unconfounded randomization in the exposures of interest; see Davey Smith et al. (2020) for more discussion on the motivation for MR.

Originally, Davey Smith and Ebrahim (2003) recognized that MR is best justified in a within-family design with parent-offspring trios. MR is commonly described as being analogous to a randomized controlled trial with non-compliance. This analogy is based on exact randomization in the transmission of alleles from parents to offspring which can be viewed as a form of treatment assignment. From its inception, it was recognized that data limitations would largely restrict MR to be performed in samples of unrelated individuals, which Davey Smith and Ebrahim (2003) termed “approximate MR”. Such approximate MR has indeed become the norm, seen in the majority of applied studies and methodological development to date. However, MR in unrelated individuals lacks the explicit source of randomization offered by the within-family design, thereby suffering potential biases from dynastic effects, population structure and assortative mating (Davies et al., 2019; Brumpton et al., 2020; Howe et al., 2022).

In addition to random assignment of exposure-modifying genetic variants, another crucial assumption for MR, known as the exclusion restriction, is that the causal effects of these variants on the outcome must be fully mediated by the exposure. When this assumption holds, MR can be framed as a special case of instrumental variable analysis (Thomas and Conti, 2004; Didelez and Sheehan, 2007). Within this framework, there has been considerable recent methodological work to replace the exclusion restriction with more plausible assumptions, typically by placing structure on the distribution of pleiotropic effects across individual genetic variants (Kang et al., 2016; Bowden, Davey Smith and Burgess, 2015; Zhao et al., 2020); see also Kolesár et al. (2015) for a similar idea in the econometrics literature.

1.2. Towards an almost exact inference for MR

As parent-offspring trio data become more widely available, it is increasingly feasible to perform MR within families, as originally proposed by [Davey Smith and Ebrahim \(2003\)](#). There has been some recent methodological development for within-family designs ([Davies et al., 2019](#); [Brumpton et al., 2020](#)). Thus far this has consisted of extensions of traditional MR techniques in which structural models for the gene-exposure and gene-outcome relationships are proposed and samples are assumed to be drawn according to these models from some large population. In particular, [Brumpton et al. \(2020\)](#) propose a linear structural model with parental genotype fixed effects. Their inference is based on this model and so the role of meiotic randomization is only implicit.

However, one of the unique advantages of MR as a natural experimental design is that it has an explicit inferential basis, namely the exogenous randomness in meiosis and fertilization, which has been thoroughly studied and modelled in genetics since at least [Haldane \(1919\)](#). Haldane developed a simple model for recombination during meiosis that has demonstrated good performance on multiple pedigrees across many species. The connection between this meiosis model and causal inference in parent-offspring trio studies was recently described in the context of locating causal genetic variants ([Bates et al., 2020](#)) and was implicit in earlier pedigree-based methods, such as the genetic linkage analysis in [Morton \(1955\)](#) and the transmission disequilibrium test in [Spielman, McGinnis and Ewens \(1993\)](#). [Lauritzen and Sheehan \(2003\)](#) attempted to represent meiosis using graphical models; however, they focused on computational considerations and did not explore the potential of these models for causal inference.

The idea of the significance test (or hypothesis test, although some authors distinguish the use of these two terms) dates back to Fisher’s original proposal for randomized experiments and is well illustrated in his famous ‘lady tasting tea’ example ([Fisher, 1935](#)). [Pitman \(1937\)](#) appears to be the first to fully embrace the idea of randomization tests. This mode of reasoning is usually referred to as randomization inference or design-based inference to contrast with model-based inference. With the aid of the potential outcome framework ([Neyman, 1990](#); [Rubin, 1974](#)), we can construct an exact randomization test for the sharp null hypothesis by conditioning on all the potential outcomes ([Rubin, 1980](#); [Rosenbaum and Rubin, 1983](#)). Randomization tests are widely used in a variety of settings, including genetics ([Spielman, McGinnis and Ewens, 1993](#); [Bates et al., 2020](#)), clinical trials ([Rosenberger, Uschner and Wang, 2019](#)), program evaluation ([Heckman and Karapakula, 2019](#)) and instrumental variable analysis ([Rosenbaum, 2004](#); [Kang, Peck and Keele, 2018](#)).

1.3. Our contributions

In this article, we propose a statistical framework that enables researchers to use meiosis models as the “reasoned basis” for inference in MR. We propose a randomization test that is *almost exact* in the sense that the test would have exactly the nominal size if the model for meiosis and fertilization were perfect. As detailed below, our methodological development in Section 3 combines several important ideas in the literature.

Our first contribution is a theoretical description of MR and its assumptions in Section 3.1 via the language of causal directed acyclic graphs (DAGs) ([Spirites, Glymour and Scheines, 2000](#); [Pearl, 2009](#)). These graphical tools allow us to visualize and dissect the assumptions imposed on an MR study. In particular, we show how various biological and social processes, including population stratification, gamete formation, fertilization, genetic linkage, assortative mating, dynastic effects, and pleiotropy, can be represented using a DAG and how they can introduce bias in MR analyses. Furthermore, by using single world intervention graphs (SWIGs) ([Richardson and Robins, 2013](#)), we identify sufficient confounder adjustment sets to eliminate these sources of bias in Section 3.2. Our

results further provide theoretical insights into a fundamental trade-off between statistical power and eliminating pleiotropy-induced bias.

For statistical inference, we propose in Section 3.3 a randomization test by connecting two existing literatures. The first literature concerns randomization inference for instrumental variable analyses, which usually assumes that the instrumental variables are randomized according to a simple design (such as random sampling of a binary instrument without replacement) (Rosenbaum, 2004; Kang, Peck and Keele, 2018). However, in MR, offspring genotypes are very high-dimensional and are randomized based on the parental haplotypes. The second literature attempts to identify the approximate location of (“map”) causal genetic variants by modelling the meiotic process (Morton, 1955; Spielman, McGinnis and Ewens, 1993; Bates et al., 2020). In Sections 3.4 to 3.6, we consider some practical issues with the randomization tests. In particular, we show how the hidden Markov model for meiosis and fertilization implied by Haldane (1919) can greatly simplify the sufficient adjustment sets and the computation of our randomization test.

In addition to the considerable conceptual advantages, our almost exact MR approach has several practical advantages too. First, unlike model-based approaches for within-family MR (Brumpton et al., 2020), our approach does not rely on a correctly specified phenotype model. Nonetheless, the randomization test can take advantage of a more accurate phenotype model to increase its power. Second, Haldane’s hidden Markov model implies a propensity score for each genetic instrument given a sufficient adjustment set (Rosenbaum and Rubin, 1983). This can be used as a “clever covariate” (Rose and van der Laan, 2008) to build powerful test statistics with attractive robustness properties. Third, since the randomization test is exact, it is robust to arbitrarily weak instruments. For an “irrelevant” instrument which induces no variation in the exposure, the test will simply have no power. Finally, by taking advantage of the DAG representation and using a sufficient confounder adjustment set, our method is also provably robust to biases arising from population structure (including multi-ancestry samples), assortative mating, dynastic effects and pleiotropy by linkage.

In Sections 4 and 5, we demonstrate the practicality of the almost exact approach to MR with a simulation study and a real data example from the Avon Longitudinal Study of Parents and Children (ALSPAC). The simulation study confirms that the randomization test is exact under the null and explores the power of the test in a number of scenarios. The applied examples consists of a negative control and a positive control. The negative control is the effect of child’s body mass index (BMI) at age 7 on mother’s BMI pre-pregnancy. Although a causal effect is temporally impossible, the existence of confounders (a.k.a. backdoor paths) may lead to false rejections of the null. The positive control is the effect of child’s BMI on itself plus some noise. We compare our results with the results from a “standard” MR analysis that does not condition on parental or offspring haplotypes. We conclude with some further discussion in Section 6.

Throughout the paper, we use i to index the parent-offspring trio (or just the offspring) and j to indicate a genomic locus. Bold font is used to represent vectors and script font is used for sets.

2. Background

2.1. Causal inference preliminaries

We will express our model and assumptions about almost exact MR using causal diagrams, then demonstrate that a randomization test for instrumental variables is a natural vehicle for inference in within-family MR. As such, a good grasp of these concepts is required to understand the remainder of the article. This section lays out some standard notation in causal inference. A lengthier introduction to the causal inference concepts used in this article—including causal graphical models, single

world intervention graphs, randomization inference, and instrumental variables—can be found in Appendix A.

Suppose we have a collection of N individuals indexed by $i = 1, 2, \dots, N$ and, among these individuals, we are interested in the effect of an exposure D_i on an outcome Y_i . For example, the exposure could be the level of alcohol consumption over some period of time and the outcome could be the incidence of cardiovascular disease. Individual i 's *potential* (or *counterfactual*) *outcomes* corresponding to exposure level $D_i = d$ are given by $Y_i(d)$. We make the *consistency* assumption (Hernán and Robins, 2020) which states that the observed outcome corresponds to the potential outcome at the realized exposure level $Y_i = Y_i(D_i)$.

Note that, in denoting the potential outcomes as $Y_i(d)$, we have implicitly made the so-called *stable unit treatment value assignment* (SUTVA) assumption (Rubin, 1980; Imbens and Rubin, 2015). That is, we have assumed that there is *no interference* in the sense that the potential outcomes of each individual are unaffected by the exposures of other individuals. We have also assumed that there are no hidden versions of the same exposure; this could be violated, for example, if the effect of alcohol consumption on cardiovascular disease has a dose-response relationship but the exposure D_i is only a binary indicator of alcohol consumption.

Potential outcomes may also be defined from a nonparametric structural equation model associated with a causal diagram using recursive substitution (Pearl, 2009). In such diagrams, vertices are used to represent random variables and directed edges are used to represent direct causal influences. The graphical and potential outcomes approaches to causal inference can be nicely unified via the single world intervention graphs (Richardson and Robins, 2013). A brief review of this can be found in the Appendix.

2.2. Genetic preliminaries

Before proceeding to present our model of within-family MR, it is also instructive to provide a basic overview of some relevant concepts in human genetics, with a focus on processes in genetic inheritance such as *meiosis* and *fertilization*. For a thorough exposition on statistical models for pedigree data, see Thompson (2000).

Human somatic cells consist of 23 pairs of chromosomes, with one in each pair inherited from the mother and the other from the father. To simplify the discussion we will only consider autosomal (non-sexual) chromosomes. Each chromosome is a doubled strand of helical DNA composed of complementary nucleotide base pairs. A base pair which exhibits population-level variation in its nucleotides is called a *single nucleotide polymorphism* (SNP). DNA sequences are typically characterized by detectable variant forms induced by different combinations of SNPs. These variant forms are called *alleles*. In this article, we will only consider variants with two alleles. A set of alleles on one chromosome inherited together from the same parent is called a *haplotype* and the unordered pair of haplotypes at the same locus is called a *genotype*.

Meiosis is a type of cell division that results in reproductive cells (a.k.a. gametes) containing one copy of each chromosome. During this process, homologous chromosomes line up and exchange segments of DNA between themselves in a biochemical process called *crossover*. The recombined chromosomes are then further divided and separated into gametes. Since recombinations are infrequent (roughly one to four per chromosome), SNPs located nearby on the same parental chromosome are more likely to be transmitted together, resulting in *genetic linkage*. Fertilization is the process by which gametes in the father (sperm cells) and mother (egg cells) join together to form a zygote, which will then normally develop into an embryo.

We will mainly be concerned with genetic trio studies, in which we observe the haplotypes of the mother, father and their child at p loci. Let $\mathcal{J} = \{1, 2, \dots, p\}$ be the set of SNP indices. In our

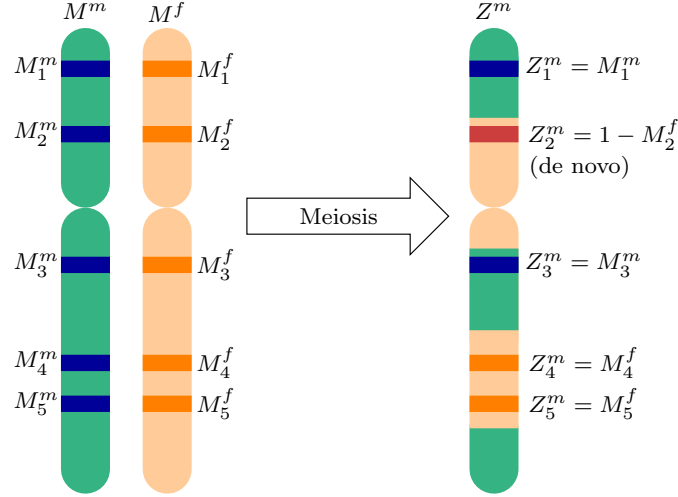


Fig 1: Illustration of the meiotic process with five loci on a chromosome.

discussion below we will assume that the SNPs are on a single chromosome, as different chromosomes are usually modelled independently. We will denote the haplotypes as follows:

offspring's haplotypes: $\mathbf{Z}^m = (Z_1^m, \dots, Z_p^m)$ and $\mathbf{Z}^f = (Z_1^f, \dots, Z_p^f)$,
 mother's haplotypes: $\mathbf{M}^m = (M_1^m, \dots, M_p^m)$ and $\mathbf{M}^f = (M_1^f, \dots, M_p^f)$, and
 father's haplotypes: $\mathbf{F}^m = (F_1^m, \dots, F_p^m)$ and $\mathbf{F}^f = (F_1^f, \dots, F_p^f)$,

where the superscript m (or f) indicates a maternally (or paternally) inherited haplotype. We only consider SNPs with two alleles, so each of the six haplotype vectors above is in $\{0, 1\}^p$. Furthermore, let $\mathbf{M}_j^{mf} = (M_j^m, M_j^f)$ denote the mother's haplotypes at locus j and similarly for \mathbf{F}_j^{mf} and \mathbf{Z}_j^{mf} . The offspring's genotype at locus $j \in \mathcal{J}$ is given by $Z_j = Z_j^m + Z_j^f$ and let $\mathbf{Z} = \mathbf{Z}^m + \mathbf{Z}^f \in \{0, 1, 2\}^p$ denote the vector of offspring genotypes.

Figure 1 illustrates how an offspring's maternally-inherited haplotype \mathbf{Z}^m at five loci on a chromosome are related to the mother's haplotypes \mathbf{M}^m and \mathbf{M}^f . In a gamete produced by meiosis, the allele at locus $j \in \mathcal{J}$ is inherited from either the mother's maternal haplotype or father haplotype (excluding mutations). This can be formalized as an ancestry indicator, $U_j^m \in \{m, f\}$. The classical meiosis model of Haldane (1919) assumes that $\mathbf{U}^m = (U_1^m, \dots, U_p^m)$ follows a (discretized) homogeneous Poisson process. Haldane's model is described in Appendix B in detail and can simplify the randomization test considerably (Section 3.5). Nonetheless, our "almost exact" approach to MR is modular and does not rely on a specific meiosis model. In fact, it is theoretically straightforward to incorporate more sophisticated meiosis models that allow for "interference" between the crossovers (Otto and Payseur, 2019). As the meiosis model become more accurate, our test will become closer to exact randomization inference.

The description in the last paragraph does not take genetic mutation into account. Many meiosis models, such as the one in Haldane (1919), assume that there is a small probability of independent mutations:

Assumption 1. Given mother's haplotypes \mathbf{M}_j^{mf} , the ancestry indicator U_j^m , and that fertilization

occurs (this is represented as $S = 1$ in Section 3),

$$Z_j^m = \begin{cases} M_j^{(U_j^m)}, & \text{with probability } 1 - \epsilon, \\ 1 - M_j^{(U_j^m)}, & \text{with probability } \epsilon. \end{cases}$$

The same model holds for the paternally-inherited haplotypes.

The rate of *de novo* mutation ϵ is about 10^{-8} in humans (Acuna-Hidalgo, Veltman and Hoischen, 2016). When only one generation is considered (as in a genetic trip study), it often suffices to treat $\epsilon = 0$ (i.e. no mutation) for practical purposes, unless it is desirable to obtain the exact randomization distribution under a recombination model.

The above meiosis model assumes no *transmission ratio distortion*. Transmission ratio distortion occurs when one of the two parental alleles is passed on to the (surviving) offspring at more or less than the expected Mendelian rate of 50% (Davies et al., 2019). Transmission ratio distortion falls into two categories: segregation distortion, when processes during meiosis or fertilization select certain alleles more frequently than others, and viability selection, when the viability of zygotes themselves depend on the offspring genotype. We sidestep this discussion for now and return to it in Section 6.

3. Almost exact Mendelian randomization

Returning to the alcohol and cardiovascular disease example in Section 2.1, observational studies suggest that moderate alcohol consumption confers reduced risk relative to abstinence or heavy consumption (Millwood et al., 2019). However, this could be a result of systematic differences among people with different drinking patterns (confounding) rather than a causally protective effect of moderate drinking. For this reason, Mendelian randomization has become a popular study design to investigate the long-term health effects of alcohol drinking (Chen et al., 2008).

The *ALDH2* gene regulates acetaldehyde metabolism and is often used as an instrumental variable for alcohol consumption. In East Asian populations, an allele of *ALDH2* produces a protein that is inactive in metabolising acetaldehyde, causing flushing and discomfort while drinking and thereby reducing consumption. Thus, we might like to use the random allocation of variant copies of *ALDH2* as the basis of causal inference. To this end, we need to carefully clarify the conditions under which this inference would be valid.

3.1. A causal model for Mendelian inheritance

Next, we construct a general graphical model to describe the process of Mendelian inheritance and genotype-phenotype relationships. This causal model allows us to identify sources of bias in within-family MR and construct sufficient adjustment sets to control for them. Under this causal model, the central idea behind almost exact MR is to base statistical inference precisely on randomness in genetic inheritance via a model for meiosis and fertilization.

Figure 2 shows a working example of our causal model on a hypothetical chromosome with $p = 3$ variants. The directed acyclic graph is structured in roughly chronological order from left to right, where A describes the population structure, S is an indicator for mating, and C is any environmental confounder between the exposure D and outcome Y .

At first glance, Figure 2 appears to be quite complicated but, by the modularity of graphical models, it can be decomposed into a collection of much simpler subgraphs that describe different

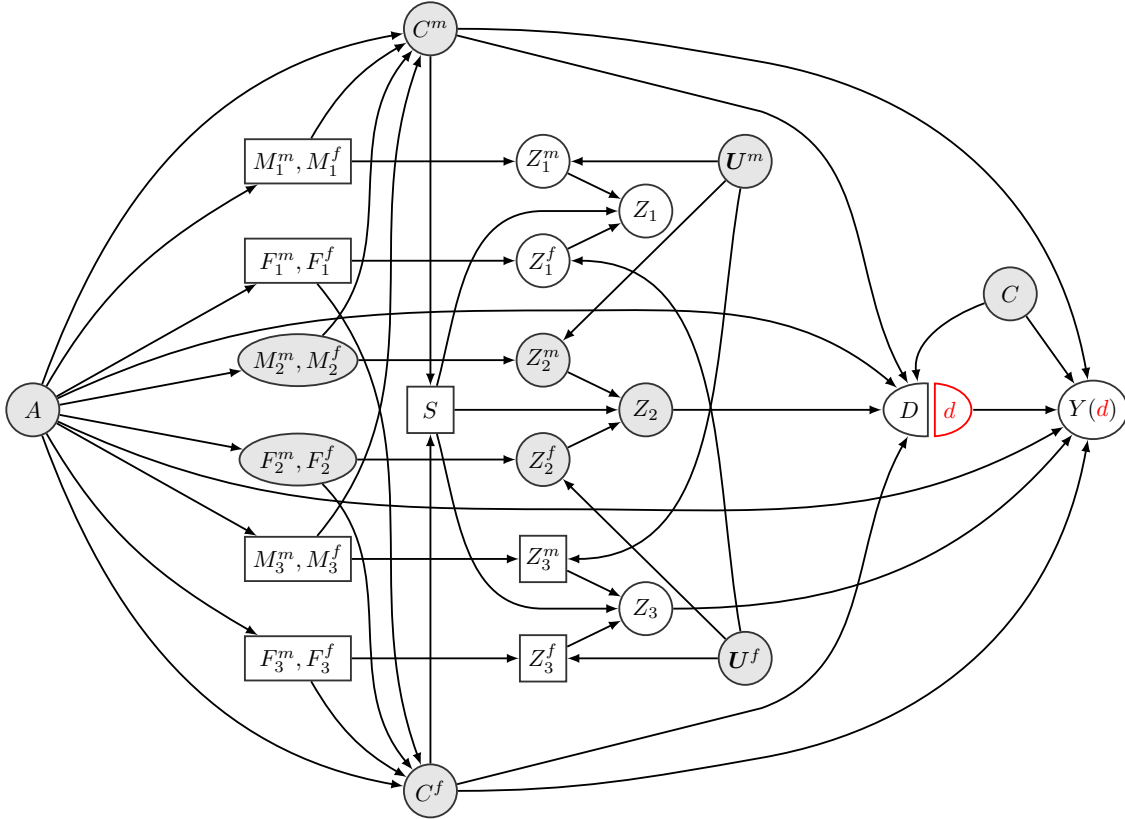


Fig 2: The single world intervention graph for a working example of a chromosome with $p = 3$ variants. Transparent nodes are observed and grey nodes are unobserved. Square nodes are the confounders being conditioned on in Proposition 2. A is ancestry; $\mathbf{M}^f = (M_1^f, M_2^f, M_3^f)$ is the mother's haplotype inherited from her father; $\mathbf{M}^m, \mathbf{F}^m$, and \mathbf{F}^f are defined similarly; C^m and C^f are generic phenotypes of the mother and father; S is an indicator of mating; $\mathbf{Z}^m = (Z_1^m, Z_2^m, Z_3^m)$ is the offspring's maternal haplotype and \mathbf{U}^m is a meiosis indicator; \mathbf{Z}^f and \mathbf{U}^f are defined similarly; $\mathbf{Z} = (Z_1, Z_2, Z_3)$ is the offspring's genotype; D is the exposure of interest; $Y(d)$ is the potential outcome of Y under the intervention that sets D to d ; C is an environmental confounder between D and Y .

TABLE 1

Factorization of the joint density of all variables in Figure 2 (p is used as a generic symbol for density functions).

Terms	Interpretation	More detail
$p(A)p(\mathbf{U}^m)p(\mathbf{U}^f)p(C)$	Exogenous variables	
$p(\mathbf{M}^m, \mathbf{M}^f A)p(\mathbf{F}^m, \mathbf{F}^f A)$	Population stratification	Section 3.1.1
$p(C^m A, \mathbf{M}^m, \mathbf{M}^f)p(C^f A, \mathbf{F}^m, \mathbf{F}^f)$	Parental phenotypes	Section 3.1.2
$p(\mathbf{Z}^m \mathbf{M}^m, \mathbf{M}^f, \mathbf{U}^m)p(\mathbf{Z}^f \mathbf{F}^m, \mathbf{F}^f, \mathbf{U}^f)$	Meiosis	Section 3.1.3
$p(S C^m, C^f)$	Assortative mating	Section 3.1.3
$p(\mathbf{Z} \mathbf{Z}^m, \mathbf{Z}^f, S)$	Fertilization	Section 3.1.3
$p(D A, \mathbf{Z}, C^m, C^f, C)p(Y(d) A, \mathbf{Z}, C^m, C^f, C)$	Offspring phenotypes, dynastic effect, confounding	Section 3.1.4

biological processes (Figure 3). By definition, a joint distribution *factorizes* according to the DAG in Figure 2 if its density function can be decomposed as described in Table 1.

Next, we describe each term in Table 1 and what this factorization implies about our assumptions on the biological processes. To simplify the discussion, we assume all DAGs in this article are faithful, so conditional independence between random variables is equivalent to d-separation in the DAG.

3.1.1. Parental genotypes

We assume that parental genotypes originate from some arbitrary, latent population structure. Population stratification is a phenomenon characterized by systematic differences in the distribution of alleles among subgroups of a population. These disparities typically emerge from social and genetic mechanisms including non-random mating, migration patterns and ‘founder effects’ (Cardon and Palmer, 2003) and can often be detected by principal component analysis (Patterson, Price and Reich, 2006). Population stratification can introduce spurious associations between genetic variants and traits (Lander and Schork, 1994).

We represent population structure via a latent node A in Figures 2 and 3a. The arrows from A to $\mathbf{M}^m, \mathbf{M}^f$ and $\mathbf{F}^m, \mathbf{F}^f$ indicate that the distribution of parental haplotypes depends on the latent population structure:

$$A \not\perp (\mathbf{M}^m, \mathbf{M}^f, \mathbf{F}^m, \mathbf{F}^f).$$

The node A may also capture any linkage disequilibrium in the parental haplotypes. That is, because the parental haplotypes are determined by the same process as the grandparental haplotypes and so on, recombination introduces dependence among nearby genetic variants (see Section 3.1.3 below for more discussion). The precise distribution of A and the conditional distribution of the parental haplotypes given A are not important below, because an appropriate subset of the parental haplotypes will be conditioned on and any paths that involve edges from A to $\mathbf{M}^m, \mathbf{M}^f, \mathbf{F}^m$, and \mathbf{F}^f will be blocked.

3.1.2. Parental phenotypes

We impose no assumptions on the nature and the distribution of the parental phenotypes C^m and C^f . They can depend arbitrarily on the parental haplotypes $\mathbf{M}^m, \mathbf{M}^f, \mathbf{F}^m, \mathbf{F}^f$ and the population structure A :

$$C^m \not\perp (A, \mathbf{M}^m, \mathbf{M}^f), \quad C^f \not\perp (A, \mathbf{F}^m, \mathbf{F}^f).$$

It is not necessary to model such dependence because the almost exact approach to MR conditions on appropriate parental haplotypes.

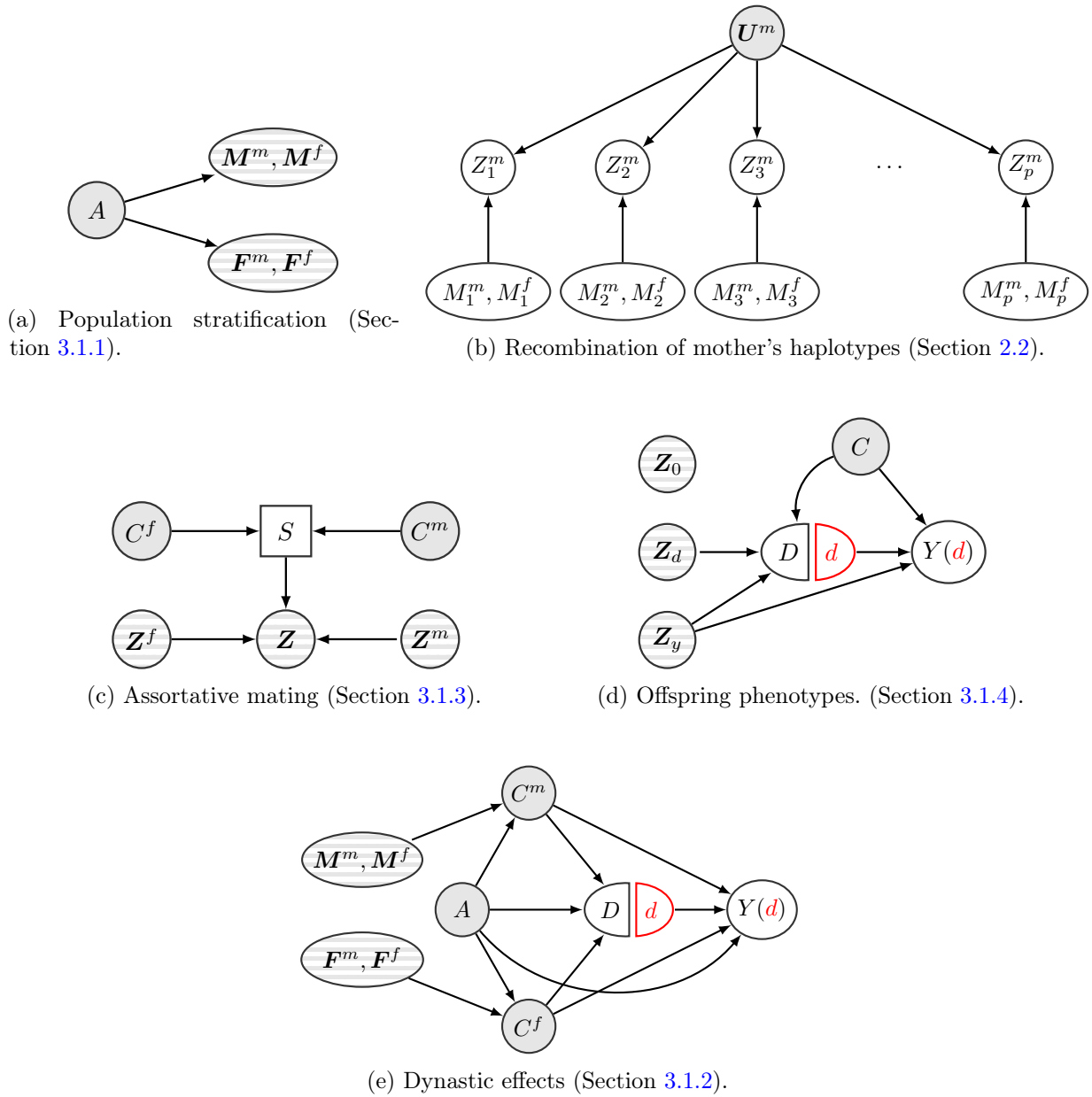


Fig 3: The constituent subgraphs of our within-family Mendelian randomization model. White nodes represent observed variables; grey nodes represent unobserved variables; and striped nodes represent variables for which some elements may be unobserved.

3.1.3. Offspring genotypes

There are two biological processes involved in the genesis of the offspring’s genotypes: meiosis (gamete formation) and fertilization. The meiotic process has been reviewed in Section 2.2, and the key Assumption 1 can be represented by the causal diagram in Figure 3b (for just the mother). A crucial assumption underlying almost exact MR is the exogeneity of the meiosis indicators U^m and U^f . This is reflected in Figures 2 and 3b, as U^m and U^f have no parents and their only children are the offspring’s haplotypes. Formally, we assume:

Assumption 2. The meiosis indicators are independent of parental haplotypes and phenotypes and any other confounders:

$$(U^m, U^f) \perp\!\!\!\perp (A, C^m, C^f, C, M^m, M^f, F^m, F^f).$$

Many stochastic processes have been proposed to model the distribution of the ancestry indicator U^m ; see Otto and Payeur (2019) for a recent review. Due to the dependence in U^m , nearby alleles on the same chromosome tend to be inherited together. This phenomenon is known as *genetic linkage*. In Section 2.2, we have described the classical model of Haldane (1919) which assumes U^m follows a Poisson process, which was used by Bates et al. (2020) to map causal variants. We will see in Section 3.5 that the Markov properties of a Poisson process greatly simplify randomization inference.

Another mechanism that needs to be modeled is fertilization. In Mendelian inheritance, it is assumed that the potential gametes (sperms and eggs) come together at random. However, mating may not be a random event. *Assortative mating* refers to the phenomenon where individuals are more likely to mate if they have complementary phenotypes. For example, there is evidence in UK Biobank that variant forms of the *ADH1B* gene related to alcohol consumption are more likely to be shared among spouses than non-spouses (Howe et al., 2019). This suggests assortative mating on drinking behaviour and may introduce bias to MR studies on alcohol consumption (Hartwig, Davies and Davey Smith, 2018).

The subgraph describing assortative mating is shown in Figure 3c, where the mating indicator $S \in \{0, 1\}$ is dependent on the parental phenotypes C^m and C^f . Any MR study necessarily conditions on $S = 1$, otherwise the offspring would not exist and the trio data would not be available. This is formalized in Figure 3c by the arrows from S to Z . In particular, we may define the offspring’s genotype Z as

$$Z = \begin{cases} Z^m + Z^f, & \text{if } S = 1, \\ \text{Undefined}, & \text{if } S = 0. \end{cases} \quad (1)$$

Notice that the above definition recognizes the fact that the gametes Z^m and Z^f are produced regardless of whether fertilization actually takes place.

Finally, the assumption of no transmission ratio distortion is formalized by the absence of arrows from Z^m and Z^f to S . This is not necessarily a benign assumption, given empirical evidence that gametes may pair up non-randomly (Nadeau, 2017).

Assumption 3. There is no transmission ratio distortion in the sense that

$$S \perp\!\!\!\perp (Z^m, Z^f) \mid (M^{mf}, F^{mf}).$$

3.1.4. Offspring phenotypes

Finally, we describe assumptions on the offspring phenotypes. We are interested in estimating the causal effect of an offspring phenotype $D \in \mathcal{D} \subseteq \mathbb{R}$ on another offspring phenotype $Y \in \mathcal{Y} \subseteq \mathbb{R}$. We

refer to D as the exposure variable and Y as the outcome variable. These phenotypes are determined by the offspring genotypes and environmental factors (including parental traits). For a particular realization of the genotypes \mathbf{z} , we denote the counterfactual exposure as $D(\mathbf{z})$. Furthermore, under an additional intervention that sets D to d , we denote the counterfactual outcome as $Y(\mathbf{z}, d)$. These potential outcomes are related to the observed data tuple (\mathbf{Z}, D, Y) by

$$D = D(\mathbf{Z}), Y = Y(\mathbf{Z}, D) = Y(\mathbf{Z}, D(\mathbf{Z})),$$

which is a simple extension of the consistency assumption (12) before.

We are interested in making inference about the counterfactuals $Y(d) = Y(\mathbf{Z}, d)$ when the exposure is set to $d \in \mathcal{D}$. As the exposure D typically varies according to the population structure, parental phenotypes and other environmental factors, it is not randomized in the sense that

$$Y(d) \not\perp\!\!\!\perp D \text{ for some or all } d \in \mathcal{D}.$$

For example, if D is alcohol consumption and Y is cardiovascular disease, there may exist offspring confounders such as diet or smoking habits which are common causes of both D and Y . The exact nature of the confounders is not very important for MR as it tries to use unconfounded randomness (in \mathbf{U}^m and \mathbf{U}^f) to make causal inference.

It will be helpful to categorize the genetic variants based on whether they have direct causal effects on D and/or Y .

Assumption 4. The set $\mathcal{J} = \{1, \dots, p\}$ of genetic variants can be partitioned as $\mathcal{J} = \mathcal{J}_y \cup \mathcal{J}_d \cup \mathcal{J}_0$, where

- \mathcal{J}_y includes all *pleiotropic* variants with a direct causal effect on Y not mediated by D (some of which may have a causal effect on D as well).
- \mathcal{J}_d includes all causal variants for D with no direct effect on Y .
- $\mathcal{J}_0 = \mathcal{J} \setminus (\mathcal{J}_y \cup \mathcal{J}_d)$ includes all other variants.

In our working example in Figure 2, $\mathcal{J}_y = \{3\}$, $\mathcal{J}_d = \{2\}$, and $\mathcal{J}_0 = \{1\}$. If the exposure D indeed has a causal effect on the outcome Y , the loci of the causal variants of Y are given by $\mathcal{J}_y \cup \mathcal{J}_d$.

For subscripts $s \in \{0, d, y\}$, we let $\mathbf{Z}_s = \{Z_j : j \in \mathcal{J}_s\}$ denote the corresponding genotypes, which has support $\mathcal{Z}_s = \{0, 1, 2\}^{|\mathcal{J}_s|}$. By Assumption 4, our potential outcomes can be written as (with an abuse of notation)

$$D(\mathbf{z}) = D(\mathbf{z}_d), Y(\mathbf{z}, d) = Y(\mathbf{z}_y, d), Y(\mathbf{z}) = Y(\mathbf{z}_y, D(\mathbf{z}_d)) = Y(\mathbf{z}_y, \mathbf{z}_d),$$

where $\mathbf{z} = (\mathbf{z}_d, \mathbf{z}_y, \mathbf{z}_0) \in \mathcal{Z}_d \times \mathcal{Z}_y \times \mathcal{Z}_0 = \mathcal{Z}$ and $d \in \mathcal{D}$.

Figure 3d provides the graphical representation of Assumption 4. Each element of \mathbf{Z}_0 has no effect on D or $Y(d)$, each element of \mathbf{Z}_d has an effect on D and each element of \mathbf{Z}_y has an effect on $Y(d)$ (some are also causes of D). The vector \mathbf{Z}_y contains the so-called pleiotropic variants that are causally involved in the expression of multiple phenotypes (Hemani, Bowden and Davey Smith, 2018). Universal pleiotropy is assumed in the famous infinitesimal model of Fisher (1918). Currently, the widely accepted view is that pleiotropy is at least widespread and some have argued for a omnigenic model (Boyle, Li and Pritchard, 2017).

Dynastic effects, sometimes called *genetic nurture* (Kong et al., 2018), is a phenomenon characterized by parental genotypes exerting an influence on the offspring's phenotypes via the parental phenotypes. This is depicted in Figure 3e, where paths emanate from the parental haplotypes \mathbf{M}^{mf} and \mathbf{F}^{mf} to the parental phenotypes C^m and C^f and on to the offspring phenotypes D and Y .

3.2. Conditions for identification

With the causal model outlined in Section 3.1 in mind, we now describe some sufficient conditions under which some $Z_j \in \mathbf{Z}$ is a valid instrumental variable for estimating the causal effect of D on Y . Recall that an instrumental variable induces unconfounded variation in the exposure without otherwise affecting the outcome. Due to population stratification (Figure 3a), assortative mating (Figure 3c), and dynastic effects (Figure 3e), the offspring genotypes \mathbf{Z} as a whole are usually not properly randomized without conditioning on the parental haplotypes. That is,

$$\mathbf{Z} \not\perp\!\!\!\perp D(\mathbf{z}), Y(\mathbf{z}, d) \text{ for some or all } \mathbf{z} \in \mathcal{Z} \text{ and } d \in \mathcal{D}.$$

To restore validity of genetic instruments, the key idea is to condition on the parental haplotypes as envisioned by Davey Smith and Ebrahim (2003) and used in the context of gene mapping by Spielman, McGinnis and Ewens (1993) and Bates et al. (2020). This allows us to use precisely the exogenous randomness in the ancestry indicators \mathbf{U}^m and \mathbf{U}^f that occurs during meiosis and fertilization. This idea is formalized in the next proposition.

Proposition 1. *Under the causal graphical model described in Section 3.1, the offspring's maternal haplotype Z_j^m (or genotype Z_j) at some site $j \in \mathcal{J}$ is independent of all ancestral and offspring confounders given the maternal (or parental) haplotypes at site j :*

$$Z_j^m \perp\!\!\!\perp (A, C^m, C^f, C) \mid (\mathbf{M}_j^{mf}, S = 1), \quad Z_j \perp\!\!\!\perp (A, C^m, C^f, C) \mid (\mathbf{M}_j^{mf}, \mathbf{F}_j^{mf}, S = 1). \quad (2)$$

However, the conditional independence (2) alone does not guarantee the validity of Z_j as an instrumental variable. The main issue is that Z_j might be in linkage disequilibrium with other causal variants of Y . Our goal is to find a set of variables \mathbf{V} such that Z_j is conditionally independent of the potential outcome $Y(d)$. This is formalized in the definition below.

Definition 1. We say a genotype Z_j is a *valid instrumental variable* given \mathbf{V} (for estimating the causal effect of D on Y) if the following conditions are satisfied:

1. Relevance: $Z_j \not\perp\!\!\!\perp D \mid \mathbf{V}$;
2. Exogeneity: $Z_j \perp\!\!\!\perp Y(d) \mid \mathbf{V}$ for all $d \in \mathcal{D}$;
3. Exclusion restriction: $Y(z_j, d) = Y(d)$ for all $z_j \in \{0, 1, 2\}$ and $d \in \mathcal{D}$.

Similarly, we say a haplotype Z_j^m is a valid instrument given \mathbf{V} if the same conditions above hold with Z_j replaced by Z_j^m and $z_j \in \{0, 1, 2\}$ replaced by $z_j^m \in \{0, 1\}$.

In our setup (Assumption 4), the exclusion restriction is satisfied if and only if $j \notin \mathcal{J}_y$.

To gain intuition on how the set of variables \mathbf{V} can be selected, it is helpful to return to the working example in Figure 2. We see that Z_3 does not satisfy the exclusion restriction because Z_3 has a direct effect on Y . The causal variant Z_2 for D would be a valid instrument if we condition on the corresponding haplotypes and Z_3 , but Z_2 is not observed in this example. This leaves us with one remaining candidate instrument: Z_1 (and potentially its haplotypes Z_1^m and Z_1^f). The relevance assumption is satisfied as long as \mathbf{V} does not block both of the following paths

$$\begin{aligned} Z_1 &\leftarrow Z_1^m \leftarrow \mathbf{U}^m \rightarrow Z_2^m \rightarrow Z_2 \rightarrow D; \\ Z_1 &\leftarrow Z_1^f \leftarrow \mathbf{U}^f \rightarrow Z_2^f \rightarrow Z_2 \rightarrow D. \end{aligned}$$

The exclusion restriction is satisfied because Z_1 is not a causal variant for Y . Finally, exogeneity is satisfied if \mathbf{V} blocks the path

$$\begin{aligned} Z_1 &\leftarrow Z_1^m \leftarrow \mathbf{U}^m \rightarrow Z_3^m \rightarrow Z_3 \rightarrow Y(d); \\ Z_1 &\leftarrow Z_1^f \leftarrow \mathbf{U}^f \rightarrow Z_3^f \rightarrow Z_3 \rightarrow Y(d). \end{aligned}$$

TABLE 2
Some paths between Z_1 and $Y(d)$ in Figure 2.

Name of bias	Example path	Blocking variable
Dynastic effect	$Z_1^m \leftarrow \mathbf{M}_1^{mf} \rightarrow C^m \rightarrow Y(d)$	\mathbf{M}_1^{mf}
Population stratification	$Z_1^m \leftarrow \mathbf{M}_1^{mf} \leftarrow A \rightarrow Y(d)$	\mathbf{M}_1^{mf}
Pleiotropy	$Z_1^m \leftarrow \mathbf{U}^m \rightarrow Z_3^m \rightarrow Z_3 \rightarrow Y(d)$	Z_3^m or Z_3
Assortative mating	$Z_1^m \leftarrow \mathbf{M}_1^{mf} \leftarrow C^m \rightarrow \boxed{S} \leftarrow$ $\leftarrow C^f \leftarrow \mathbf{F}_3^{mf} \rightarrow Z_3^f \rightarrow Z_3 \rightarrow Y(d)$	\mathbf{M}_1^{mf} , Z_3 , or \mathbf{F}_3^{mf}
Nearly determined ancestry	$Z_1^m \leftarrow \mathbf{U}^m \rightarrow \boxed{Z_3^m} \leftarrow \mathbf{M}_3^{mf} \rightarrow C^m \rightarrow Y(d)$	\mathbf{M}_3^{mf}

Thus, we have the following result:

Proposition 2. *For the example in Figure 2, the following conditional independence relationships are true for all $d \in \mathcal{D}$:*

$$Z_1^m \perp\!\!\!\perp Y(d) \mid (\mathbf{M}_1^{mf}, \mathbf{V}_3^m, S = 1), \quad (3)$$

$$Z_1 \perp\!\!\!\perp Y(d) \mid (\mathbf{M}_1^{mf}, \mathbf{F}_1^{mf}, \mathbf{V}_3, S = 1), \quad (4)$$

where $\mathbf{V}_3^m = (\mathbf{M}_3^{mf}, Z_3^m)$ and $\mathbf{V}_3 = (\mathbf{M}_3^{mf}, \mathbf{F}_3^{mf}, Z_3)$. The adjustment variables above are minimal in the sense that no subsets of them satisfy the same conditional independence.

Proof. The conditional independence follows almost immediately from our discussion above. It is tedious but trivial to show that $\mathbf{V} = (\mathbf{M}_1^{mf}, \mathbf{V}_3^m)$ is minimal for (3). Table 2 lists the key backdoor paths between Z_1^m and $Y(d)$, describes the corresponding biological mechanism and shows how conditioning on \mathbf{V} blocks these paths. The table only includes the maternal paths, but the same blocking also holds for the corresponding paternal paths. \square

Remark 1. To our knowledge, the bias-inducing path in the last row of Table 2, which we term “nearly determined ancestry bias”, has not yet been identified in the literature. This is a form of collider bias introduced because the ancestry indicator can often be almost perfectly determined if we are given the mother’s haplotypes and the offspring’s maternal haplotype. For example, if the mother is heterozygous $M_3^m = 1, M_3^f = 0$ and the offspring’s maternal haplotype is $Z_3^m = 1$, then we know that $U_3^m = m$ is true with an extremely high confidence. Due to genetic linkage, there is also an exceedingly high probability that $U_1^m = m$, inducing dependence between the potential instrument Z_1^m with maternal haplotypes \mathbf{M}_3^{mf} . This further challenges the widely adopted hypothesis that mapping causal variants is equivalent to testing conditional independence; in our example, Z_3 is the only causal variant of $Y(d)$, but $Z_1 \perp\!\!\!\perp Y(d) \mid Z_3$ may not be true even if there is no population stratification and no causal effect from \mathbf{M}_1^{mf} on $Y(d)$.

We conclude this section with a sufficient condition for the validity of Z_j^m and Z_j in our general setting. To simplify the exposition, let $\mathbf{V}_B^m = (\mathbf{M}_B^{mf}, \mathbf{Z}_B^m)$ be a set of maternal adjustment variables, where $B \subseteq \mathcal{J} \setminus \{j\}$ is a subset of loci. Furthermore, let $\mathbf{V}_B = (\mathbf{M}_B^{mf}, \mathbf{F}_B^{mf}, \mathbf{Z}_B)$.

Theorem 1. *Suppose $\mathbf{Z} = (Z_1, \dots, Z_p)$ is a full chromosome. Consider the general causal model for Mendelian randomization in Section 3.1 and let $j \in \mathcal{J}$ be the index of a candidate instrument. Then Z_j^m is a valid instrument conditional on $(\mathbf{M}_j^{mf}, \mathbf{V}_B^m)$ if the following conditions are satisfied:*

1. $Z_j^m \not\perp\!\!\!\perp \mathbf{Z}_d^m \mid (\mathbf{M}_j^{mf}, \mathbf{V}_B^m, S = 1)$;

$$2. Z_j^m \perp\!\!\!\perp Z_y^m \mid (\mathbf{M}_j^{mf}, \mathbf{V}_{\mathcal{B}}^m, S = 1);$$

Proof. The relevance of Z_j^m follows from the first condition, because Z_j^m is dependent on some causal variants (or is itself a causal variant) of D . The exclusion restriction ($j \notin \mathcal{J}_y$) follows directly from the second condition. For exogeneity, paths from Z_j^m to $Y(d)$ either go through the confounders A , C^f , C^m , or C , which are blocked by \mathbf{M}_j^{mf} by Proposition 1, or through some causal variants of the outcome as in $Z_j^m \leftarrow \mathbf{U}^m \rightarrow \mathbf{Z}_y^m \rightarrow \mathbf{Z}_y \rightarrow Y(d)$, which are blocked by the second condition. \square

It is straightforward to extend Theorem 1 to establish validity of the genotype Z_j at locus j as an instrumental variable. Details are omitted.

Since Proposition 1 ensures that, after conditioning on \mathbf{M}_j^{mf} , the instrument Z_j^m is independent of all ancestral and offspring confounders (A, C^m, C^f, C), the only remaining threats to the validity of Z_j^m are irrelevance and pleiotropy. The set \mathcal{B} is chosen to ensure that Z_j^m is independent of all pleiotropic variants conditional on $\mathbf{V}_{\mathcal{B}}^m$ (condition 2 of Theorem 1) but not independent of the set of causal variants (condition 1 of Theorem 1).

This highlights an intrinsic trade-off in choosing the adjustment set $\mathbf{V}_{\mathcal{B}}$: by choosing a larger subset \mathcal{B} , the second condition is more likely but the first condition is less likely to be satisfied. The reason is that, when conditioning on more genetic variants, we are more likely to block the pleiotropic paths to Y but we are also more likely to block the path between the instrument and the causal variant.

For now, we will continue our discussion under the assumption that an appropriate set \mathcal{B} can be chosen. In Section 3.5, we will return to this and describe a simple construction of \mathcal{B} using Markov properties in Haldane's model for meiosis.

3.3. Hypothesis testing

We are now ready to describe the randomization-based inference for within-family Mendelian randomization. We will focus on the simplest case where a single genetic variant from the offspring's maternally-inherited haplotype is used as an instrumental variable and defer the discussion on multiple instruments to Section 3.6.

Suppose we observe N trios of parent and offspring and within each trio the observed variables can be described by the causal diagram described in Section 3.1. Let $i \in \{1, \dots, N\}$ be the index of the trio. Following Rosenbaum and Rubin (1983), we define the *propensity score* of the instrument Z_{ij}^m at locus j of individual i as

$$\pi_{ij}^m = \mathbb{P}(Z_{ij}^m = 1 \mid \mathbf{M}_{ij}^{mf}, \mathbf{V}_{i\mathcal{B}}^m) \quad (5)$$

where $\mathcal{B} \subseteq \mathcal{J}$ is an appropriately chosen set of loci that satisfies the conditions in Theorem 1. In words, π_{ij}^m describes the randomization distribution of the haplotype Z_{ij}^m conditional on a set of parental and offspring haplotypes or genotypes. For now, we will treat π_{ij}^m as known.

Let us consider the following model for the potential outcomes that assumes a constant treatment effect β :

$$Y_i(d) = Y_i(0) + \beta d \text{ for all } d \in \mathcal{D} \text{ and } i = 1, \dots, N. \quad (6)$$

Let $\mathcal{F} = \{Y_i(0): i = 1, \dots, N\}$ denote the collection of potential outcomes for all individuals i under no exposure $d = 0$. Our goal is to test null hypotheses of the form

$$H_0: \beta = \beta_0, \quad H_1: \beta \neq \beta_0 \quad (7)$$

where β_0 is some hypothetical value of the causal effect. If the null hypothesis is true, equation (6) implies that the potential outcome under no exposure ($d = 0$) can be identified from the observed data by

$$Y_i(0) = Y_i(D_i) - \beta_0 D_i = Y_i - \beta_0 D_i.$$

For ease of notation, let $Q_i(\beta_0) = Y_i - \beta_0 D_i$ be the adjusted outcome.

Theorem 2 and the model (6) imply that we are essentially testing the following conditional independence:

$$H_0: Z_{ij}^m \perp\!\!\!\perp Q_i(\beta_0) \mid (\mathbf{M}_{ij}^{mf}, \mathbf{V}_{iB}^m) \quad \text{vs.} \quad H_1: Z_{ij}^m \not\perp\!\!\!\perp Q_i(\beta_0) \mid (\mathbf{M}_{ij}^{mf}, \mathbf{V}_{iB}^m). \quad (8)$$

Let $\mathbf{Z}_j^m = (Z_{1j}^m, \dots, Z_{Nj}^m)$ and similarly define other vector-valued genotypes. Suppose we have selected a test statistic $T(\mathbf{Z}_j^m \mid \mathcal{F})$ whose dependence on $(\mathbf{M}_j^{mf}, \mathbf{V}_B^m)$ is implicit. For example, this could be the coefficient from a regression of the adjusted outcome on the instrument. The randomization-based p-value for H_0 can then be written as

$$\begin{aligned} P(\mathbf{Z}_j^m \mid \mathcal{F}) &= \tilde{\mathbb{P}}(T(\tilde{\mathbf{Z}}_j^m \mid \mathcal{F}) \leq T(\mathbf{Z}_j^m \mid \mathcal{F})) \\ &= \sum_{\tilde{\mathbf{z}}^m \in \{0,1\}^N} I\{T(\tilde{\mathbf{z}}^m \mid \mathcal{F}) \leq T(\mathbf{Z}_j^m \mid \mathcal{F})\} \prod_{i=1}^N (\pi_{ij}^m)^{\tilde{z}_i} (1 - \pi_{ij}^m)^{1 - \tilde{z}_i}, \end{aligned} \quad (9)$$

where $I\{\cdot\}$ is the indicator function, $\tilde{\mathbf{Z}}_j^m$ denotes an independent, random draw from (5) and $\tilde{\mathbb{P}}$ denotes its probability distribution. Given the propensity score and the null hypothesis, this p-value can be computed exactly by enumerating over all 2^N possible values of $\tilde{\mathbf{Z}}^m$, or using a Monte Carlo approximation by drawing a large sample of $\tilde{\mathbf{Z}}^m$ using the propensity scores π_j^m ; see Algorithm 1 for the pseudo-code. It is straightforward to replace the haplotype Z_{ij}^m with the genotype Z_{ij} ; the randomization distribution of $Z_{ij} \in \{0, 1, 2\}$ is a simple function of π_{ij}^m and π_{ij}^f since meioses in the mother and father are independent.

Equation (9) highlights the importance of the vector π_j^m of propensity scores in randomization inference. However, π_j^m describes a biochemical process occurring in the human body which is not precisely known to, or controlled by, us. Therefore, the best we can do is perform *almost exact* inference by replacing π_j^m with an accurate approximation. The model we use in this paper is Haldane’s hidden Markov model described in Appendix B. As discussed in Section 2.2 our method is modular in the sense that more sophisticated meiosis models can easily be substituted as the randomization distribution; see Broman and Weber (2000); Otto and Payseur (2019) for discussion and comparison of alternative models.

3.4. Choice of test statistic

Our randomization test retains the nominal size under the null hypothesis, regardless of the choice of the test statistic. Nonetheless, a well chosen statistic may substantially increase the power of the test. A practical challenge is that the adjustment set $(\mathbf{M}_j^{mf}, \mathbf{V}_B)$ may be high-dimensional and highly correlated, and their role in designing the test statistic is unclear. We propose to use the following “clever covariate” in the test statistic:

$$X_{ij}^m = \frac{Z_{ij}^m}{\pi_{ij}^m} - \frac{1 - Z_{ij}^m}{1 - \pi_{ij}^m}.$$

Algorithm 1: Almost exact test

Compute the test statistic on the observed data $t = T(\mathbf{Z}_j^m \mid \mathcal{F})$;
for $k = 1, \dots, K$ **do**
 Sample a counterfactual instrument $\tilde{\mathbf{Z}}_j^m$ from the randomization distribution (e.g. using Theorem 3 in Appendix B based on Haldane’s model);
 Compute the test statistic using the counterfactual instrument $\tilde{t}_k = T(\tilde{\mathbf{Z}}_j^m \mid \mathcal{F})$;
end
Compute an approximation to the p-value in Equation (9) via the proportion of $\tilde{t}_1, \dots, \tilde{t}_K$ which are larger than t :

$$\hat{P}(\mathbf{Z}_j^m \mid \mathcal{F}) = \frac{|\{k: t \leq \tilde{t}_k\}|}{K}.$$

We may then use the weighted difference-in-means statistic

$$T(\mathbf{Z}_j^m \mid \mathcal{F}) = \sum_{i=1}^N Q_i(\beta_0) X_{ij}^m$$

or the F -statistic in a linear regression of $Q_i(\beta_0)$ on Z_{ij}^m and X_{ij}^m . A simulation example in Section 4.2 shows that using this clever covariate can increase the power of the test dramatically.

The idea of using a “clever covariate” is proposed in Scharfstein, Rotnitzky and Robins (1999) and Rose and van der Laan (2008) and is commonly used in semiparametric estimators of the average treatment effect. Heuristically, the clever covariate exploits the so-called “central role” of the propensity score (Rosenbaum and Rubin, 1983): $Y_i(d) \perp\!\!\!\perp Z_{ij}^m \mid \pi_{ij}^m$, provided that $0 < \pi_{ij}^m < 1$. Thus, the propensity score π_{ij}^m may be viewed as a one-dimensional summary of the sufficient adjustment set $(\mathbf{M}_{ij}^{mf}, \mathbf{V}_{iB})$ and is particularly convenient here because it can be directly computed from a meiosis model.

3.5. Simplification via Markovian structure

Thus far, we have sidestepped the issue of choosing the adjustment set \mathbf{V}_B and computing the propensity score. Conditional independencies implied by Haldane’s meiosis model allows us to greatly simplify the sufficient confounder adjustment set. We explain this below.

The conditions in Theorem 1 are trivially satisfied with $\mathcal{B} = \emptyset$ if $\mathcal{J}_y = \emptyset$ and $\mathcal{J}_d \neq \emptyset$, i.e., all causal variants of Y on this chromosome only affect Y through D . However, this is a rather unlikely situation. More often, we need to condition on some variants to block the pleiotropic paths (such as Z_3 in the working example in Figure 2). To this end, we can utilize the Markovian structure on the meiosis indicators \mathbf{U}^m and \mathbf{U}^f implied by Haldane’s model. Roughly speaking, such structure implies that

$$Z_j \perp\!\!\!\perp Z_l \mid (\mathbf{M}_j^{mf}, \mathbf{F}_j^{mf}, \mathbf{V}_k) \text{ for all } j < k < l,$$

if there are no mutations and mother’s genotype at locus k is heterozygous (i.e. $M_k^f \neq M_k^m$).

More generally, let b_1 and b_2 ($b_1 < j < b_2$) be two heterozygous loci in the mother’s genome, i.e., $M_{b_1}^f \neq M_{b_1}^m$ and $M_{b_2}^f \neq M_{b_2}^m$. Let $\mathcal{A} = \{b_1 + 1, \dots, b_2 - 1\}$ be the set of loci between b_1 and b_2 , which of course contains the locus j of interest.

Theorem 2. Consider the setting in Theorem 1 and suppose

1. The meiosis indicator process is a Markov chain so that $U_j^m \perp\!\!\!\perp U_l^m \mid U_k^m$ for all $j < k < l$;
2. There are no mutations: $\epsilon = 0$.

Then Z_j^m is a valid instrumental variable conditional on $(\mathbf{M}_j^{mf}, \mathbf{V}_{\{b_1, b_2\}}^m)$ if the following conditions are true: 3. $\mathcal{A} \cap \mathcal{J}_d \neq \emptyset$; 4. $\mathcal{A} \cap \mathcal{J}_y = \emptyset$.

Proof. Because there are no mutations and M_{b_1} and M_{b_2} are heterozygous, we can uniquely determine $U_{b_1}^m$ and $U_{b_2}^m$ from $\mathbf{V}_{\{b_1, b_2\}}^m$. By the assumed Markovian structure, this means that

$$Z_j^m \perp\!\!\!\perp Z_l^m \mid \mathbf{M}_j^{mf}, \mathbf{V}_{\{b_1, b_2\}}^m \text{ for all } j < b_1 \text{ or } j > b_2.$$

Thus, the last two conditions in Theorem 2 imply the two conditions in Theorem 1. \square

One can easily mirror the above result for using the paternal haplotype Z_j^f as an instrument variable. Furthermore, let b'_1 and b'_2 ($b'_1 < j < b'_2$) be two heterozygous loci in the father's genome. Then it is easy to see that $Z_j = Z_j^m + Z_j^f$ is a valid instrument conditional on $(\mathbf{M}_j^{mf}, \mathbf{F}_j^{mf}, \mathbf{V}_{\{b_1, b_2\}}^m, \mathbf{V}_{\{b'_1, b'_2\}}^f)$ if the last two conditions hold for the union $\mathcal{A} = \{\min(b_1, b'_1) + 1, \dots, \max(b_2, b'_2) - 1\}$.

Under the setting in Theorem 2, we can partition the offspring genome into mutually independent subsets by conditioning on heterozygous parental genotypes. This partition is useful for constructing independent p-values when we have multiple instruments. Suppose we have a collection of genomic position $\mathcal{B} = \{b_1, \dots, b_k\}$ that will be conditioned on and let $\mathcal{A}_k = \{b_{k-1} + 1, \dots, b_k - 1\}$ be the loci in between (suppose $b_0 = 0$ and $b_{k+1} = p + 1$). This induces the following partition of the chromosome:

$$\mathcal{J} = \mathcal{A}_1 \cup \{b_1\} \cup \mathcal{A}_2 \cup \{b_2\} \cup \dots \cup \mathcal{A}_k \cup \{b_k\} \cup \mathcal{A}_{k+1}. \quad (10)$$

Proposition 3. *Suppose $M_j^m \neq M_j^f$ for all $j \in \mathcal{B}$. Then, under the first two assumptions in Theorem 2, we have*

$$Z_j^m \perp\!\!\!\perp Z_{j'}^m \mid (\mathbf{M}_j^{mf}, \mathbf{M}_{j'}^{mf}, \mathbf{V}_{\mathcal{B}}^m).$$

for any $j \in \mathcal{A}_l$ and $j' \in \mathcal{A}_{l'}$ such that $l \neq l'$.

Proof. The proof follows from an almost identical argument to Theorem 1. The assumption that $\epsilon = 0$ means that U_j^m is uniquely determined for all $j \in \mathcal{B}$ from \mathbf{M}_j^{mf} and Z_j^m . Therefore the assumed Markovian structure implies that conditioning on $\mathbf{V}_{\mathcal{B}}^m$, along with the parental haplotypes \mathbf{M}_j^{mf} and $\mathbf{M}_{j'}^{mf}$, then induces the conditional independence. \square

3.6. Multiple instruments

Proposition 3 allows us to formalize the intuition that genetic instruments across the genome may provide independent pieces of evidence.

Corollary 1. *Suppose $j \in \mathcal{A}_l$, $j' \in \mathcal{A}_{l'}$, and $l \neq l'$. Then Z_j^m and $Z_{j'}^m$ are independent, valid instruments given $(\mathbf{M}_j^{mf}, \mathbf{M}_{j'}^{mf}, \mathbf{V}_{\mathcal{B}}^m)$ if*

1. The first two assumptions of Theorem 2 hold;
2. $\mathcal{A}_l \cap \mathcal{J}_d \neq \emptyset$ and $\mathcal{A}_{l'} \cap \mathcal{J}_d \neq \emptyset$;
3. $\mathcal{A}_l \cap \mathcal{J}_y = \emptyset$ and $\mathcal{A}_{l'} \cap \mathcal{J}_y = \emptyset$.

Corollary 1 says that any two instruments are valid and independent if they lie in separate regions in the partition (10) and each region contains at least one causal variant of the exposure and no pleiotropic variants (i.e. variants with a direct effect on Y not mediated by D).

As a direct application of this corollary, we can use standard procedures to combine randomization p-values obtained from different genetic instruments and test the null hypothesis (see e.g. [Bretz, Hothorn and Westfall, 2016](#)). One such procedure is Fisher's method ([Fisher, 1925](#)): let $\{p_1, p_2, \dots, p_k\}$

be a collection of independent p-values, then $-2 \sum_{j=1}^k \log(p_j) \sim \chi_{2k}^2$ when all of the corresponding null hypotheses are true. We will use this method to aggregate p-values in the applied example in Section 5.

As some instruments may violate the exclusion restriction, a more robust approach is to test the partial conjunction of the null hypotheses (Benjamini and Heller, 2008; Wang and Owen, 2019); loosely speaking, this means that we reject the causal null hypothesis only if quite a few genetic instruments appear to provide evidence against it.

As a final remark, it may be impossible in practice to separate closely linked instruments into partitions separated by a heterozygous variant, in which case the hypothesis (8) can be tested using $(Z_j^m, Z_{j'}^m)$ jointly. Corollary 3 in Appendix C derives the joint randomization distribution of a collection of instruments.

4. Simulation

4.1. Setup and illustration

In this section we explore the properties of our almost exact test via a numerical simulation. The set up of the simulation is described in detail in Appendix D. To summarize, we generate a dataset of 15,000 parent-offspring trios with a null effect of an exposure on an outcome (i.e. $\beta = 0$), both of which have variance one, and consider 5 genetic instruments on a chromosome with $p = 150$ loci. The instruments are non-causal markers for nearby causal variants and there are also pleiotropic variants in linkage disequilibrium with the instruments.

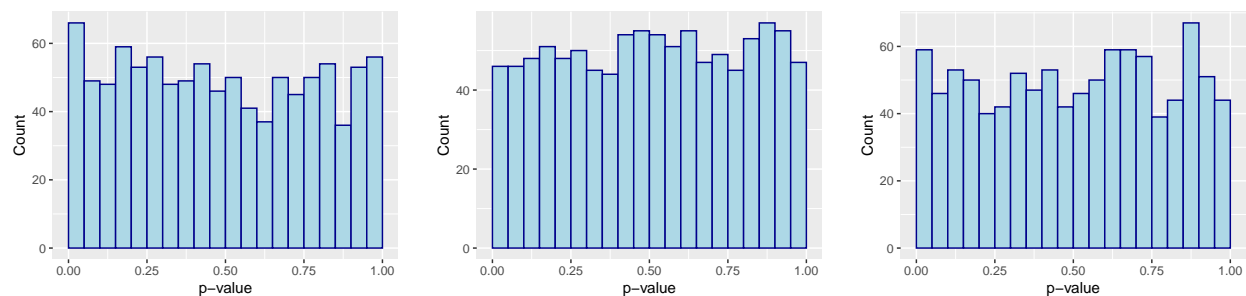
4.2. Power

We now use the simulation to study the power of the randomization test, assuming a correct adjustment set is used (see Equation (23) in Appendix D). As the haplotypes are simulated according to Haldane’s meiosis model, the randomization test should be exact. This is verified by the near-uniform distributions of the p-values for testing the correct null hypothesis $H_0 : \beta = 0$ with three different test statistics in the top panels of Figure 4.

The histograms in the bottom panels of Figure 4 depict the distribution of p-values for a test of a false null hypothesis $H_0 : \beta = 0.5$. The power of the test varies significantly according to the choices of test statistic. The simple F -statistic based on a linear regression of the adjusted outcome on the instruments (test statistic 1) has almost no power, while the test statistic obtained from the same model but with the propensity score included as a clever covariate (test statistic 2) has a reasonable power of about 0.52.

Figure 5 expands upon the previous figure by plotting a power curve for each test statistic. We can see that test statistic 1 has almost no power between $\beta_0 = 0$ and $\beta_0 = 1$. Since test statistic 1 is unconditional on the adjustment set, resampled offspring haplotypes retain their correlation with the confounders via the parental haplotypes. This can cause under-rejection of false null hypotheses around the unconditional instrumental variable estimator. In this simulation, the Anderson-Rubin 95% confidence interval is 0.64–0.89, which aligns with the region of under-rejection.

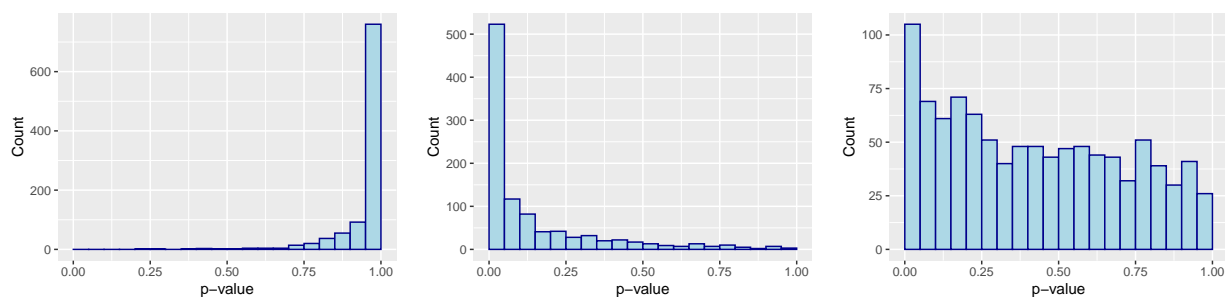
Test statistic 2, on the other hand, conditions on the confounders via a clever covariate. It has a power curve that is centred on the true null $\beta_0 = 0$ and has significantly improved power in the region between $\beta_0 = 0$ and $\beta_0 = 1$. However, it should be noted that test statistic 2 is not uniformly more powerful than test statistic 1.



(a) $H_0 : \beta = 0$ (true) and test statistic 1.

(b) $H_0 : \beta = 0$ (true) and test statistic 2.

(c) $H_0 : \beta = 0$ (true) and test statistic 3.



(d) $H_0 : \beta = 0.5$ (false) and test statistic 1.

(e) $H_0 : \beta = 0.5$ (false) and test statistic 2.

(f) $H_0 : \beta = 0.5$ (false) and test statistic 3.

Fig 4: Histograms of 1,000 p-values for several null hypotheses and test statistics. Test statistic 1 is the F-statistic from a linear regression of the adjusted outcome on the instruments. Test statistic 2 includes the propensity scores for each instrument as covariates. Test statistic 3 includes the parental haplotypes as covariates.

5. Applied example

5.1. Preliminaries

We illustrate our approach with a pair of negative and positive controls using the Avon Longitudinal Study of Parents and Children (ALSPAC). Our dataset consists of 6,222 mother-child duos from ALSPAC, a longitudinal cohort initially comprising pregnant women resident in Avon, UK with expected dates of delivery from 1 April 1991 to 31 December 1992. The initial sample consisted of 14,676 fetuses, resulting in 14,062 live births and 13,988 children who were alive at 1 year of age. In subsequent years, mothers, children and occasionally partners attended several waves of questionnaires and clinic visits, including genotyping. For a more thorough cohort description, see [Boyd et al. \(2013\)](#) and [Fraser et al. \(2013\)](#).¹

The negative control is the effect of child’s BMI at age 7 on mother’s BMI pre-pregnancy. Dynastic effects, as depicted in Figure 3e, could induce a spurious correlation between child’s BMI-associated variants and their mother’s BMI pre-pregnancy. Blocking this backdoor path is crucial for reliable causal inference. The positive control is the effect of child’s BMI at age 7 on a simulated, noisy version of itself. We vary the proportion of the outcome that is attributable to noise to assess the power of our test.

5.2. Data processing

We use ALSPAC genotype data generated using the Illumina HumanHap550 chip (for children) and Illumina human660W chip (for mothers) and imputed to the 1000 Genomes reference panel. We remove SNPs with missingness of more than 5% and minor allele frequency of less than 1%. Haplotypes are phased using the `SHAPEIT2` software with the `duoHMM` flag, which ensures that phased haplotypes are consistent with known pedigrees in the sample. We obtain recombination probabilities from the 1000 Genomes genetic map file on Genome Reference Consortium Human Build 37.

Our instruments are selected from the genome-wide association study (GWAS) of [Vogelezang et al. \(2020\)](#), which identifies 25 genetic variants for childhood BMI, including 2 novel loci located close to *NEDD4L* and *SLC45A3*. Of the genome-wide significant variants in the discovery sample, we select 11 with a p-value of less than 0.001 in the replication sample. ALSPAC is included in the discovery sample, so independent replication is important for avoiding spurious associations with the exposure. Two of our instruments, rs571312 and rs76227980, are located close together near *MC4R* and need to be tested jointly. We exclude rs62107261 because it is not contained in the 1000 Genomes genetic map file. We condition on all variants outside of a 500 kilobase window around each instrument.

5.3. Results

Tables 3 and 4 show results for the negative and positive controls, respectively. The last row of each table shows the p-value from Fisher’s method aggregated across all independent p-values. The aggregated p-value for the negative control is 0.21, indicating little evidence against the null. The aggregated p-values for the positive control range from 0.03 (when 10% of the variance of the simulated outcome is noise) to 0.16 (when 50% of the variance of the simulated outcome is noise). This indicates weak evidence against the null even when the effect is quite strong.

We can also compare the results in Tables 3 and 4 with per-instrument p-values obtained from two-stage least squares (2SLS) using the same offspring haplotypes as instruments, unconditional on

¹Please note that the study website contains details of all the data that is available through a fully searchable data dictionary and variable search tool (<https://www.bristol.ac.uk/alspac/researchers/our-data/>).

TABLE 3
Results from the ALSPAC negative control example.

Instrument (rsID)	Chromosome	Proximal gene	P-value
rs11676272	2	<i>ADCY3</i>	0.45
rs7138803	12	<i>BCDIN3D</i>	0.55
rs939584	2	<i>TMEM18</i>	0.39
rs17817449	16	<i>FTO</i>	0.06
rs12042908	1	<i>TNNI3K</i>	0.35
rs543874	1	<i>SEC16B</i>	0.07
rs56133711	11	<i>BDNF</i>	0.59
rs571312, rs76227980	18	<i>MC4R</i>	0.48
rs12641981	4	<i>GNPDA2</i>	0.62
rs1094647	1	<i>SLC45A3</i>	0.19
Fisher's method			0.21

TABLE 4
Results from the ALSPAC positive control example. (Chr. = chromosome)

Instrument (rsID)	Chr.	Gene	P-value for noise of		
			10%	20%	50%
rs11676272	2	<i>ADCY3</i>	0.01	0.01	0.01
rs7138803	12	<i>BCDIN3D</i>	0.01	0.01	0.01
rs939584	2	<i>TMEM18</i>	0.98	0.95	0.88
rs17817449	16	<i>FTO</i>	0.33	0.35	0.44
rs12042908	1	<i>TNNI3K</i>	0.77	0.79	0.85
rs543874	1	<i>SEC16B</i>	0.48	0.64	0.92
rs56133711	11	<i>BDNF</i>	0.12	0.14	0.25
rs571312, rs76227980	18	<i>MC4R</i>	0.31	0.39	0.63
rs12641981	4	<i>GNPDA2</i>	0.49	0.56	0.76
rs1094647	1	<i>SLC45A3</i>	0.23	0.25	0.35
Fisher's method			0.03	0.05	0.16

parental or other offspring haplotypes. For the negative control, the p-value from Fisher's method is 0.02, indicating some evidence against the null. This is expected, given that the backdoor paths remain unblocked. For the positive control, the p-values from Fisher's method range from less than 10^{-20} (when 10% of the variance of the simulated outcome is noise) to 4.5×10^{-11} (when 50% of the variance of the simulated outcome is noise). This indicates that the unconditional analysis has significantly more power to detect non-zero effects compared to our "almost exact" test. We discuss potential reasons for, and implications of, this low power in Section 6

6. Discussion

We have presented an almost exact approach to within-family MR, which has a number of conceptual and practical advantages over model-based approaches to MR using population GWAS data. However, the applied example in Section 5 demonstrates that power may be limited relative to conventional MR analyses in unrelated individuals. Since our test leverages the precise amount of information available in a single meiosis, this suggests that MR in unrelated individuals is drawing power from elsewhere.

Besides the obvious distinction that conventional MR analyses are model-based (and thus are

not robust to model misspecification), another likely reason for the large difference in the empirical results is that MR in unrelated individuals use randomness in meiosis across many generations. For example, an offspring with parents who are homozygous for the non-effect allele offers no power in our test, since their genotype will not vary across meioses. However, if we assume that genotypes are randomly distributed at the population level (as in MR studies with unrelated individuals), that same offspring can act as a comparator for individuals with the effect allele. [Brumpton et al. \(2020\)](#) corroborate this loss of power for their within-family method, but do not elaborate on the broader implications for how Mendelian randomization is typically justified. It would be extremely valuable for the MR literature to discuss the extent to which Mendelian inheritance across multiple generations is driving the power behind existing results, as such uncontrolled randomness may introduce bias when there are strong dynastic effects and natural selection.

Continuing the discussion on multiple instruments in Section 3.6, our approach closely resembles the usage of evidence factors in observational studies as advocated by [Rosenbaum \(2010, 2021\)](#) and [Zhao et al. \(2022\)](#). Using (conditionally) independent instruments in different genomic regions may also be viewed as a form of triangulation to improve causal inference ([Lawlor, Tilling and Davey Smith, 2017](#)). Although all the p-values are obtained using the same study design, different genetic variants may influence the exposure through different biological mechanisms and the fact that they provide corroborating evidence strengthens the causal conclusion.

We must also return to the problem of transmission ratio distortion (TRD) discussed in Section 2.2. TRD violates the assumptions of our meiosis model that alleles are (unconditionally) passed from parents to offspring at the Mendelian rate of 50%. We could represent TRD in our causal model in Figure 2 via an arrow from the gametes (Z^m, Z^f) to the mating indicator S . This indicates that the gametes themselves influence survival of their corresponding zygote to term. If our putative instrument Z_1^m is in linkage with any variant exhibiting TRD, then this invalidates it as an instrument. Suppose Z_3^m exhibits TRD, then this opens collider paths via the parental phenotypes C^m and C^f , for example, $Y(d) \leftarrow C^m \rightarrow \boxed{S} \leftarrow Z_3^m \leftarrow U^m \rightarrow Z_1^m$. The intuition is that parental phenotypes related to the likelihood of mating become associated with offspring variants related to the likelihood of offspring survival. Within our causal model, this pathway can be closed by conditioning on Z_3^m , with unconditioned variants obeying the meiosis model. If any unconditioned variants exhibit TRD, then this bias will remain and our meiosis model will incorrectly describe the inheritance patterns of any linked variants, resulting in an erroneous randomization distribution. Expanding resources of parent-offspring data may allow us to test the prevalence of transmission ratio distortion, which will help to inform the reasonableness of maintaining Mendel’s First Law in our meiosis and fertilization model.

Acknowledgments

The authors thank Kate Tilling, Rachael A Hughes, Jack Bowden, Gibran Hemani, Neil M Davies, Ben Brumpton, and Nianqiao Ju for their helpful feedback. In addition, the authors are extremely grateful to all the families who took part in the ALSPAC cohort, the midwives for their help in recruiting them, and the whole ALSPAC team, which includes interviewers, computer and laboratory technicians, clerical workers, research scientists, volunteers, managers, receptionists and nurses. Ethical approval for our applied example was obtained from the ALSPAC Ethics and Law Committee and the Local Research Ethics Committees. This publication is the work of the authors who will serve as guarantors for the contents of this paper. For the purpose of Open Access, the authors have applied a CC BY public copyright licence to any Author Accepted Manuscript version arising from this submission.

Funding

This research was supported in part by the Wellcome Trust (grant number 220067/Z/20/Z) and EPSRC (grant number EP/V049968/1). The UK Medical Research Council and Wellcome (grant number 217065/Z/19/Z) and the University of Bristol provide core support for ALSPAC. GWAS data was generated by Sample Logistics and Genotyping Facilities at Wellcome Sanger Institute and LabCorp (Laboratory Corporation of America) using support from 23andMe.

References

- ACUNA-HIDALGO, R., VELTMAN, J. A. and HOISCHEN, A. (2016). New insights into the generation and role of de novo mutations in health and disease. *Genome Biology* **17** 1–19.
- BATES, S., SESIA, M., SABATTI, C. and CANDÈS, E. (2020). Causal inference in genetic trio studies. *Proceedings of the National Academy of Sciences of the United States of America* **117** 24117–24126.
- BELMONT, J. W., BOUDREAU, A., LEAL, S. M., HARDENBOL, P. et al. (2005). A haplotype map of the human genome. *Nature* **437** 1299–1320.
- BENJAMINI, Y. and HELLER, R. (2008). Screening for partial conjunction hypotheses. *Biometrics* **64** 1215–1222.
- BHERER, C., CAMPBELL, C. L. and AUTON, A. (2017). Refined genetic maps reveal sexual dimorphism in human meiotic recombination at multiple scales. *Nature Communications* **8**.
- BOWDEN, J., DAVEY SMITH, G. and BURGESS, S. (2015). Mendelian randomization with invalid instruments: effect estimation and bias detection through Egger regression. *International Journal of Epidemiology* **44** 512–525.
- BOYD, A., GOLDING, J., MACLEOD, J., LAWLOR, D. A., FRASER, A., HENDERSON, J., MOLLOY, L., NESS, A., RING, S. and DAVEY SMITH, G. (2013). Cohort Profile: The ‘Children of the 90s’—the index offspring of the Avon Longitudinal Study of Parents and Children. *International Journal of Epidemiology* **42** 111–127.
- BOYLE, E. A., LI, Y. I. and PRITCHARD, J. K. (2017). An expanded view of complex traits: From polygenic to omnigenic. *Cell* **169** 1177–1186.
- BRETZ, F., HOTHORN, T. and WESTFALL, P. (2016). *Multiple Comparisons Using R*. // Chapman and Hall/CRC.
- BROMAN, K. W. and WEBER, J. L. (2000). Characterization of human crossover interference. *American Journal of Human Genetics* **66** 1911–1926.
- BRUMPTON, B., SANDERSON, E., HEILBRON, K., HARTWIG, F. P. et al. (2020). Avoiding dynastic, assortative mating, and population stratification biases in Mendelian randomization through within-family analyses. *Nature Communications* **11** 1–13.
- CARDON, L. R. and PALMER, L. J. (2003). Population stratification and spurious allelic association. *Lancet* **361** 598–604.
- CHEN, L., SMITH, G. D., HARBORD, R. M. and LEWIS, S. J. (2008). Alcohol Intake and Blood Pressure: a Systematic Review Implementing a Mendelian Randomization Approach. *PLoS Medicine* **5** e52.
- DAVEY SMITH, G. (2001). Reflections on the limitations to epidemiology. *Journal of Clinical Epidemiology* **54** 325–331.
- DAVEY SMITH, G. (2007). Capitalizing on Mendelian Randomization To Assess the Effects of Treatments. *Journal of the Royal Society of Medicine* **100** 432–435.

- DAVEY SMITH, G. and EBRAHIM, S. (2003). 'Mendelian randomization': Can genetic epidemiology contribute to understanding environmental determinants of disease? *International Journal of Epidemiology* **32** 1–22.
- DAVEY SMITH, G., HOLMES, M. V., DAVIES, N. M. and EBRAHIM, S. (2020). Mendel's laws, Mendelian randomization and causal inference in observational data: substantive and nomenclatural issues. *European Journal of Epidemiology* **35** 99–111.
- DAVIES, N. M., HOWE, L. J., BRUMPTON, B., HAVDAHL, A., EVANS, D. M. and DAVEY SMITH, G. (2019). Within family Mendelian randomization studies. *Human Molecular Genetics* **28** R170–R179.
- DIDELEZ, V. and SHEEHAN, N. (2007). Mendelian randomization as an instrumental variable approach to causal inference. *Statistical Methods in Medical Research* **16** 309–330.
- FEINSTEIN, A. R. (1988). Scientific standards in epidemiologic studies of the menace of daily life. *Science* **242** 1257–1263.
- FISHER, R. A. (1918). The Correlation Between Relatives on the Supposition of Mendelian Inheritance. *Transactions of the Royal Society of Edinburgh* **52** 399–433.
- FISHER, R. A. (1925). *Statistical methods for research workers*. Oliver & Boyd, Edinburgh.
- FISHER, R. A. (1926). The Arrangement of Field Experiments. *Journal of the Ministry of Agriculture* **33** 503–513.
- FISHER, R. A. (1935). *The design of experiments*. Oliver & Boyd, Edinburgh.
- FISHER, R. A. (1951). Statistical methods in genetics. *Heredity* **6** 1–12.
- FRASER, A., MACDONALD-WALLIS, C., TILLING, K., BOYD, A., GOLDING, J., DAVEY SMITH, G., HENDERSON, J., MACLEOD, J., MOLLOY, L., NESS, A., RING, S., NELSON, S. M. and LAWLOR, D. A. (2013). Cohort Profile: The Avon Longitudinal Study of Parents and Children: ALSPAC mothers cohort. *International Journal of Epidemiology* **42** 97–110.
- GRAY, R. and WHEATLEY, K. (1991). How to avoid bias when comparing bone marrow transplantation with chemotherapy. *Bone Marrow Transplantation* **7** 9–12.
- HALDANE, J. B. S. (1919). The combination of linkage values and the calculation of distances between the loci of linked factors. *Journal of Genetics* **8** 299–309.
- HARTWIG, F. P., DAVIES, N. M. and DAVEY SMITH, G. (2018). Bias in Mendelian randomization due to assortative mating. *Genetic Epidemiology* **42** 608–620.
- HECKMAN, J. J. and KARAPAKULA, G. (2019). The Perry Preschoolers at Late Midlife: A Study in Design-Specific Inference. *National Bureau of Economic Research Working Paper Series No. 25888* 14–21.
- HEMANI, G., BOWDEN, J. and DAVEY SMITH, G. (2018). Evaluating the potential role of pleiotropy in Mendelian randomization studies. *Human Molecular Genetics* **27** R195–R208.
- HERNÁN, M. A. and ROBINS, J. M. (2020). *Causal inference: what if*. Chapman & Hall/CRC, Boca Raton.
- HOLLAND, P. W. (1986). Statistics and causal inference. *Journal of the American Statistical Association* **81** 945–960.
- HOWE, L. J., LAWSON, D. J., DAVIES, N. M., ST. POURCAIN, B., LEWIS, S. J., DAVEY SMITH, G. and HEMANI, G. (2019). Genetic evidence for assortative mating on alcohol consumption in the UK Biobank. *Nature Communications* **10**.
- HOWE, L. J., NIVARD, M. G., MORRIS, T. T., HANSEN, A. F. et al. (2022). Within-sibship genome-wide association analyses decrease bias in estimates of direct genetic effects. *Nature Genetics* **54** 581–592.
- IMBENS, G. W. and RUBIN, D. B. (2015). *Causal Inference for Statistics, Social, and Biomedical Sciences: An Introduction*. Cambridge University Press, Cambridge.
- KANG, H., PECK, L. and KEELE, L. (2018). Inference for instrumental variables: A randomization

- inference approach. *Journal of the Royal Statistical Society. Series A: Statistics in Society* **181** 1231–1254.
- KANG, H., ZHANG, A., CAI, T. T. and SMALL, D. S. (2016). Instrumental Variables Estimation With Some Invalid Instruments and Its Application To Mendelian Randomization. *Journal of the American Statistical Association* **111** 132-144.
- KATAN, M. B. (1986). Apolipoprotein E isoforms, serum cholesterol, and cancer. *International Journal of Epidemiology* **33** 9.
- KOLEŠÁR, M., CHETTY, R., FRIEDMAN, J., GLAESER, E. and IMBENS, G. W. (2015). Identification and Inference With Many Invalid Instruments. *Journal of Business & Economic Statistics* **33** 474-484.
- KONG, A., THORLEIFSSON, G., FRIGGE, M. L., VILHJÁLMSSON, B. J., YOUNG, A. I., THORGEIRSSON, T. E., BENONISDOTTIR, S., ODDSSON, A., HALLDÓRSSON, B. V., MASSON, G., GUDBJARTSSON, D. F., HELGASON, A., BJORNSDOTTIR, G., THORSTEINSDOTTIR, U. and STEFANSSON, K. (2018). The nature of nurture: Effects of parental genotypes. *Science* **359** 424–428.
- LANDER, E. S. and SCHORK, N. J. (1994). Genetic dissection of complex traits. *Science* **265** 2037–2048.
- LAURITZEN, S. L. and SHEEHAN, N. A. (2003). Graphical models for genetic analyses. *Statistical Science* **18** 489–514.
- LAURITZEN, S. L., DAWID, P. A., LARSEN, B. N. and LEIMER, H. G. (1990). Independence properties of directed markov fields. *Networks* **20** 491–505.
- LAWLOR, D. A., TILLING, K. and DAVEY SMITH, G. (2017). Triangulation in Aetiological Epidemiology. *International Journal of Epidemiology* **nil** dyw314.
- LOWER, G. M., NILSSON, T., NELSON, C. E., WOLF, H., GAMSKY, T. E. and BRYAN, G. T. (1979). N-Acetyltransferase Phenotype and Risk in Urinary Bladder Cancer: Approaches in Molecular Epidemiology. Preliminary Results in Sweden and Denmark. *Environmental Health Perspectives* **29** 71-79.
- MILLWOOD, I. Y., WALTERS, R. G., MEI, X. W., GUO, Y., YANG, L., BIAN, Z., BENNETT, D. A., CHEN, Y., DONG, C., HU, R., ZHOU, G., YU, B., JIA, W., PARISH, S., CLARKE, R., DAVEY SMITH, G., COLLINS, R., HOLMES, M. V., LI, L., PETO, R. and CHEN, Z. (2019). Conventional and genetic evidence on alcohol and vascular disease aetiology: a prospective study of 500 000 men and women in China. *The Lancet* **393** 1831–1842.
- MORTON, N. E. (1955). Sequential tests for the detection of linkage. *American Journal of Human Genetics* **7** 277-318.
- NADEAU, J. H. (2017). Do gametes woo? Evidence for their nonrandom union at fertilization. *Genetics* **207** 369–387.
- NEYMAN, J. (1990). On the application of probability theory to agricultural experiments. Essay on principles. Section 9. *Statistical Science* **5** 465–480.
- OTTO, S. P. and PAYSEUR, B. A. (2019). Crossover interference: Shedding light on the evolution of recombination. *Annual Review of Genetics* **53** 19–44.
- PATTERSON, N., PRICE, A. L. and REICH, D. (2006). Population Structure and Eigenanalysis. *PLoS Genetics* **2** e190.
- PEARL, J. (2009). *Causality*, 2 ed. Cambridge University Press, New York.
- PITMAN, E. J. G. (1937). Significance Tests Which May Be Applied To Samples From Any Populations. *Supplement to the Journal of the Royal Statistical Society* **4** 119-130.
- RICHARDSON, T. S. and ROBINS, J. M. (2013). Single world intervention graphs (SWIGs): A unification of the counterfactual and graphical approaches to causality.
- ROSE, S. and VAN DER LAAN, M. J. (2008). Simple optimal weighting of cases and controls in case-controls studies. *The International Journal of Biostatistics* **4**.

- ROSENBAUM, P. R. (2004). Randomization inference with an instrumental variable.
- ROSENBAUM, P. R. (2010). Evidence factors in observational studies. *Biometrika* **97** 333–345.
- ROSENBAUM, P. (2021). *Replication and evidence factors in observational studies*. CRC Press.
- ROSENBAUM, P. R. and RUBIN, D. B. (1983). The central role of the propensity score in observational studies for causal effects. *Biometrika* **70** 41–55.
- ROSENBERGER, W. F., USCHNER, D. and WANG, Y. (2019). Randomization: The forgotten component of the randomized clinical trial. *Statistics in Medicine* **38** 1–12.
- RUBIN, D. B. (1974). Estimating causal effects of treatment in randomized and nonrandomized studies. *Journal of Educational Psychology* **66** 688–701.
- RUBIN, D. B. (1980). Comment: 'Randomization analysis of experimental data: The Fisher randomization test'. *Journal of the American Statistical Association* **75** 591–593.
- SANDERSON, E., GLYMOUR, M. M., HOLMES, M. V., KANG, H., MORRISON, J., MUNAFÒ, M. R., PALMER, T., SCHOOLING, M. C., WALLACE, C., ZHAO, Q. and DAVEY SMITH, G. (2022). Mendelian randomization. *Nature Reviews Methods Primers* **2**.
- SCHARFSTEIN, D. O., ROTNITZKY, A. and ROBINS, J. M. (1999). Adjusting for nonignorable drop-out using semiparametric nonresponse models. *Journal of the American Statistical Association* **94** 1096–1120.
- SPIELMAN, R. S., MCGINNIS, R. E. and EWENS, W. J. (1993). Transmission test for linkage disequilibrium: The insulin gene region and insulin-dependent diabetes mellitus (IDDM). *American Journal of Human Genetics* **52** 506–516.
- SPIRITES, P., GLYMOUR, C. N. and SCHEINES, R. (2000). *Causation, prediction, and search*. MIT press.
- TAUBES, G. (1995). Epidemiology faces its limits. *Science* **269** 164–169.
- THOMAS, D. C. and CONTI, D. V. (2004). Commentary: The concept of 'Mendelian randomization'. *International Journal of Epidemiology* **33** 21–25.
- THOMPSON, E. A. (2000). Statistical inference from genetic data on pedigrees. In *NSF-CBMS Regional Conference Series in Probability and Statistics* **6** 1–169.
- VOGELEZANG, S., BRADFIELD, J. P., AHLUWALIA, T. S., CURTIN, J. A. et al. (2020). Novel loci for childhood body mass index and shared heritability with adult cardiometabolic traits. *PLoS Genetics* 1–26.
- WANG, J. and OWEN, A. B. (2019). Admissibility in Partial Conjunction Testing. *Journal of the American Statistical Association* **114** 158–168.
- WHEATLEY, K. and GRAY, R. (2004). Commentary: Mendelian randomization - An update on its use to evaluate allogeneic stem cell transplantation in leukemia. *International Journal of Epidemiology* **33** 15–17.
- WRIGHT, S. (1920). The relative importance of heredity: determining the piebald pattern of guinea pigs. *Proceedings of the National Academy of Sciences* **6** 320–332.
- WRIGHT, S. (1923). The theory of path coefficients: a reply to Niles' criticism. *Genetics* **8** 239–255.
- ZHAO, Q., WANG, J., HEMANI, G., BOWDEN, J. and SMALL, D. S. (2020). Statistical inference in two-sample summary-data Mendelian randomization using robust adjusted profile score. *Annals of Statistics* **48** 1742–1769.
- ZHAO, A., LEE, Y., SMALL, D. S. and KARMAKAR, B. (2022). Evidence Factors From Multiple, Possibly Invalid, Instrumental Variables. *The Annals of Statistics* **50** nil.

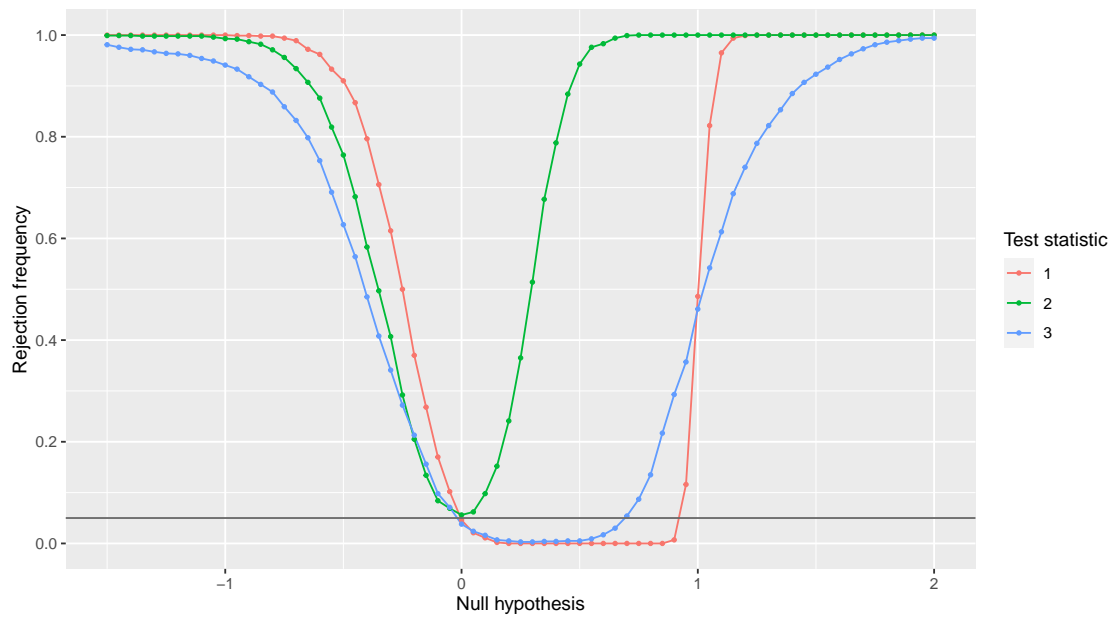


Fig 5: Power curves for the three choices of test statistic. Test statistic 1 is the F-statistic from a linear regression of the adjusted outcome on the instruments. Test statistic 2 includes the propensity scores for each instrument as covariates. Test statistic 3 includes the parental haplotypes as covariates. Each point on the figure is the rejection frequency over 1,000 replications.

Appendix A: Introduction to causal inference

This section introduces some basic concepts in causal inference, including the potential outcomes framework (Neyman, 1990; Rubin, 1974), randomization inference (Fisher, 1935; Rubin, 1980), instrumental variables (Wright, 1923; Imbens and Rubin, 2015), and single world intervention graphs (Richardson and Robins, 2013), which are essential for describing our methodology. Interested readers can find a more thorough coverage of these topics in other texts (Imbens and Rubin, 2015; Hernán and Robins, 2020).

A.1. Treatment assignment and potential outcomes

In the typical setup of a randomized experiment with non-compliance, we have a sample of N individuals indexed by $i = 1, 2, \dots, N$ and each individual is randomly assigned to receive a binary treatment $Z_i \in \{0, 1\}$. The common convention is that $Z_i = 1$ denotes assignment to an experimental treatment and $Z_i = 0$ a control treatment. However, individuals might not comply with their assigned treatment, and we denote the treatment that the individual actually takes as $D_i \in \{0, 1\}$. Finally, we observe an outcome variable Y_i for each individual. As the treatment uptake D_i is not randomized, there may exist a confounding variable C_i that is a common cause of both D_i and Y_i .

Individual i has two *potential outcomes* (also called *counterfactuals*) of her treatment uptake, $D_i(0)$ and $D_i(1)$. If she is randomized to the experimental (or control) treatment, she will take treatment $D_i(1)$ (or $D_i(0)$). For example, some individuals will take the experimental treatment regardless of their assigned treatment, so $D_i(1) = D_i(0) = 1$. Each individual also has four potential outcomes $Y_i(z, d)$ from the experiment corresponding to each combination of treatment assignment $z \in \{0, 1\}$ and treatment uptake $d \in \{0, 1\}$. Similarly, we may define the potential outcome with just D being intervened on by $Y_i(d) = Y_i(Z_i, d)$, where the assigned treatment takes its “natural” value Z_i .

In defining these potential outcomes, we have implicitly made the *no interference* assumption which states that individual j ’s treatment is independent of individual i ’s outcome when $i \neq j$ (Rubin, 1980). To simplify the exposition, we further make the *exclusion restriction* assumption in this section. That is, we assume that the treatment assignment has no causal effect on the outcome except via treatment uptake, so

$$Y_i(1, d) = Y_i(0, d) = Y_i(d) \text{ for } d \in \{0, 1\}. \quad (11)$$

Let $\mathcal{F} = \{(D_i(1), D_i(0), Y_i(0), Y_i(1)), i = 1, \dots, N\}$ denote the collection of potential outcomes for all the individuals.

We define a *causal effect* of the treatment as a contrast of potential outcomes. When the treatment is binary, the causal effect for individual i is given by $\beta_i = Y_i(1) - Y_i(0)$, the difference in individual i ’s outcomes between the two possible treatments. However, inference for the individual treatment effect β_i is difficult because we do not observe both potential outcomes of the same individual simultaneously. This has been famously described as the “fundamental problem of causal inference” (Holland, 1986). Indeed, we only observe the potential outcome corresponding to the treatment that is actually received, such that

$$D_i = \begin{cases} D_i(1) & \text{if } Z_i = 1, \\ D_i(0) & \text{if } Z_i = 0; \end{cases} \text{ and } Y_i = \begin{cases} Y_i(1) & \text{if } D_i = 1, \\ Y_i(0) & \text{if } D_i = 0. \end{cases} \quad (12)$$

The above equation is sometimes called the *consistency* assumption since it ensures that the observed outcomes and potential outcomes are consistent with one another (Hernán and Robins, 2020).

TABLE 5
Observed data from a hypothetical experiment for a LDL cholesterol-lowering drug.

i	Z_i	D_i	$D_i(1)$	$D_i(0)$	Y_i	$Y_i(1)$	$Y_i(0)$
1	1	1	1	?	120	120	?
2	1	1	1	?	120	120	?
3	1	0	0	?	75	?	75
4	0	0	?	1	165	165	?
5	0	0	?	0	135	?	135
6	0	0	?	0	105	?	105

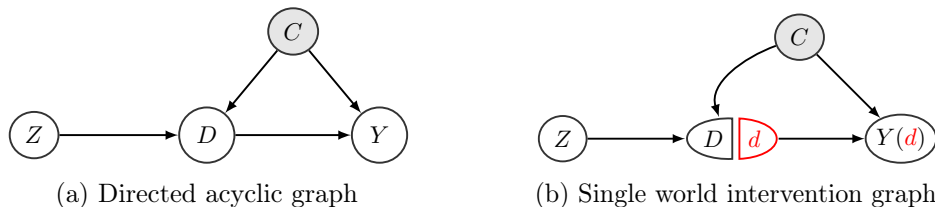


Fig 6: Causal diagram of the example in Appendix A

From this perspective, causal inference can be regarded as a missing data problem. Consider a simple hypothetical experiment in Table 5 consisting of $N = 6$ individuals, 3 of whom are randomized to take an experimental LDL cholesterol-lowering drug and 3 of whom are randomized to take a placebo. However, not everyone adheres to the assigned treatment. The outcome variable is LDL cholesterol measured in grams per litre (mg/dL). As discussed above, we can only observe the potential outcomes corresponding to the observed treatment assignment and uptake; all other potential outcomes are missing.

A.2. Causal graphical models

The setting above can be described by a directed acyclic graph (DAG) as shown in Figure 6a. Below we will use some basic concepts in DAG models such as Markov properties and d-separation, which are described in detail in other texts (Lauritzen et al., 1990; Pearl, 2009; Hernán and Robins, 2020).

We will use single world intervention graphs (SWIG) to unify the counterfactual and graphical descriptions of the causal inference problem (Richardson and Robins, 2013). The SWIG representation of our setting above is given in Figure 6b. Since we are interested in the causal effect of an intervention on D , the SWIG splits that node into two halves: D , representing the randomized treatment, and d , representing a fixed intervention value. The random half D inherits all incoming arrows in the original DAG and the fixed half d inherits all outgoing arrows. Descendants of the intervention node (in this case Y) are replaced with the potential outcomes $Y(d)$ under the intervention value d .

It has been shown that SWIGs define a graphical model for the potential outcomes (Richardson and Robins, 2013), so we can apply d-separation to obtain conditional independence between counterfactuals. For example, Figure 6b implies *exchangeability* (or *ignorability*),

$$Z_i \perp\!\!\!\perp Y_i(d) \text{ for all } d \in \{0, 1\}. \quad (13)$$

However, $D_i \perp\!\!\!\perp Y_i(d)$ is generally not true due to the confounder C_i .

A.3. Randomization inference for instrumental variables

To construct an exact randomization test, the key idea is to base the inference precisely on the randomness introduced by the experimenter. To this end, we must characterize the treatment assignment mechanism.

Let $\mathbf{Z} = (Z_1, \dots, Z_N)^\top$ denote the N -vector of treatment assignments. To simplify the exposition, we will assume that the experiment is completely randomized, such that a fixed number of individuals N_t are assigned to the experimental treatment and $N_c = N - N_t$ are assigned to the control treatment. The same method below can be applied to more sophisticated assignment mechanisms (such as the ones we describe later for within-family MR). Let $\Omega = \{(z_1, \dots, z_N) \in \{0, 1\}^N : \sum_{i=1}^N z_i = N_t\}$ denote the set of feasible assignment vectors. By assumption, all assignment vectors in Ω are realized with equal probability. Stated formally, the randomization distribution can be written as

$$\mathbb{P}(\mathbf{Z} = \mathbf{z} \mid \mathcal{F}) = \begin{cases} \binom{N}{N_t}^{-1}, & \text{for all } \mathbf{z} \in \Omega, \\ 0, & \text{otherwise.} \end{cases} \quad (14)$$

To illustrate randomization inference, consider the hypothetical experiment in Table 5. Suppose we are interested in evaluating the effectiveness of this drug at lowering LDL cholesterol. However, although the drug is initially randomly assigned, the treatment uptake is not randomized. In particular, non-compliance may be driven by a confounder $C_i \in \{0, 1\}$. This might be an underlying comorbidity such that those with $C_i = 1$ have a higher baseline outcome $Y_i(0)$ but experience negative side effects from the experimental treatment. Due to the side effects, individuals with the comorbidity (such as $i = 3$ in Table 5) may be inclined to switch to the control treatment when they are assigned to the experimental drug. Due to the systematic shift of high baseline individuals from the experimental treatment to the control treatment, a simple intention-to-treat estimate (by regressing Y_i on Z_i) will underestimate the causal effect.

To address unobserved confounding such as systematic non-compliance, one approach is to use an instrumental variable. An instrumental variable induces unconfounded variation in the treatment without otherwise affecting the outcome. In our example, the randomized treatment assignment $Z_i \in \{0, 1\}$ is a good instrument for treatment uptake D_i , because it will change the outcome Y_i only through D_i by the exclusion restriction assumption (11). Furthermore, it is independent of the underlying comorbidity status and the counterfactual outcomes, as shown by (13).

Randomization inference for instrumental variables (Rosenbaum, 2004; Kang, Peck and Keele, 2018) tests sharp null hypotheses of the form

$$H_0 : Y_i(d) - Y_i(0) = \beta_0 d, \text{ for all } d \in \{0, 1\}.$$

This implies a constant additive treatment effect β_0 across individuals. Under this hypothesis and the consistency assumption (12), the baseline potential outcome can be written in terms of the observable data (Z_i, D_i, Y_i) as

$$Y_i(0) = Y_i - \beta_0 D_i = \begin{cases} Y_i, & \text{if } D_i = 0, \\ Y_i - \beta_0, & \text{if } D_i = 1, \end{cases}$$

which is termed as the ‘‘adjusted response’’ by Rosenbaum (2004). Therefore, when the null hypothesis is true, the randomization of Z_i , namely (13), implies that

$$Z_i \perp\!\!\!\perp Y_i - \beta_0 D_i.$$

Consequently, testing the null hypothesis H_0 that the causal effect is a constant β_0 is equivalent to testing the independence of Z_i and $Y_i - \beta_0 D_i$. To this end, a simple test statistic is the difference in outcomes between the two groups,

$$T(\mathbf{Z} | \mathcal{F}) = \sum_{i=1}^N Z_i(Y_i - \beta_0 D_i) - \sum_{i=1}^N (1 - Z_i)(Y_i - \beta_0 D_i) \stackrel{H_0}{=} \sum_{i:Z_i=1} Y_i(0) - \sum_{i:Z_i=0} Y_i(0).$$

The randomization test then rejects H_0 at significance level α , if the p-value

$$P(\mathbf{Z} | \mathcal{F}) = \tilde{\mathbb{P}}(T(\tilde{\mathbf{Z}} | \mathcal{F}) \leq T(\mathbf{Z} | \mathcal{F}))$$

is less than or equal to α . Here $\tilde{\mathbf{Z}}$ is an independent copy of \mathbf{Z} and $\tilde{\mathbb{P}}$ means that the probability is taken over $\tilde{\mathbf{Z}}$ according to the randomization distribution (14). In plain terms, we are asking: if we re-ran the experiment many times under the null hypothesis (i.e. Z_i and $Y_i - \beta_0 D_i$ are independent), how often would we observe a test statistic more extreme than our observed test statistic? If this probability is lower than α , then we have little confidence in the null hypothesis.

This p-value has size α in the sense that

$$\mathbb{P}(P(\mathbf{Z} | \mathcal{F}) \leq \alpha | H_0) = \alpha.$$

for any significance level $0 \leq \alpha \leq 1$ and test statistic $T(\cdot | \mathcal{F})$. For continuously distributed test statistics the proof relies on the idea that $T(\tilde{\mathbf{Z}} | \mathcal{F}) \stackrel{d}{=} T(\mathbf{Z} | \mathcal{F})$ under H_0 which means that $P(\mathbf{Z} | \mathcal{F})$ is the cumulative distribution of $T(\tilde{\mathbf{Z}} | \mathcal{F})$ at $T(\mathbf{Z} | \mathcal{F})$. Since cumulative distributions are uniformly distributed the result follows.

Next, we illustrate the randomization test using the hypothetical experiment in Table 5 and the null hypothesis $H_0 : Y_i(0) = Y_i(1)$ for all i (i.e. $\beta_0 = 0$). For the realized experiment in Table 5, the difference in outcomes between the experimental and placebo groups is $(120 + 120)/2 - (75 + 165 + 135 + 105)/4 = 0$. In other words, average LDL cholesterol appears to be identical in the experimental and control arms. However, it is unclear whether this should be interpreted as evidence of a null causal effect. As discussed above, it is possible that individuals with high baseline outcomes are more inclined to switch from the experimental treatment to the control treatment.

Our observed test statistic for this experiment is $T(\mathbf{Z} | \mathcal{F}) = (120 + 120 + 75)/3 - (165 + 135 + 105)/3 = -30$. Since we know the missing potential outcomes under the null hypothesis and we know the mechanism by which treatment was randomly assigned, we can also consider the results of counterfactual experiments. Table 6 shows a counterfactual experiment that could have occurred with missing potential outcomes imputed under the null. The counterfactual treatment assignment is given by \tilde{Z}_i to distinguish it from the factual Z_i . We can compute the difference in outcomes from this counterfactual experiment, equal to $T(\tilde{\mathbf{Z}} | \mathcal{F}) = 420/3 - 300/3 = 40$. Indeed, we could enumerate the counterfactual results from all 20 equally possible experiments, shown in Figure 7. The bars highlighted in red are comprised of 4 counterfactual experiments with an average outcome difference less than or equal to that observed in our actual experiment. Therefore, under the null hypothesis, the one-sided probability of observing a result more extreme than our observed result is $4/20$ or 20%.

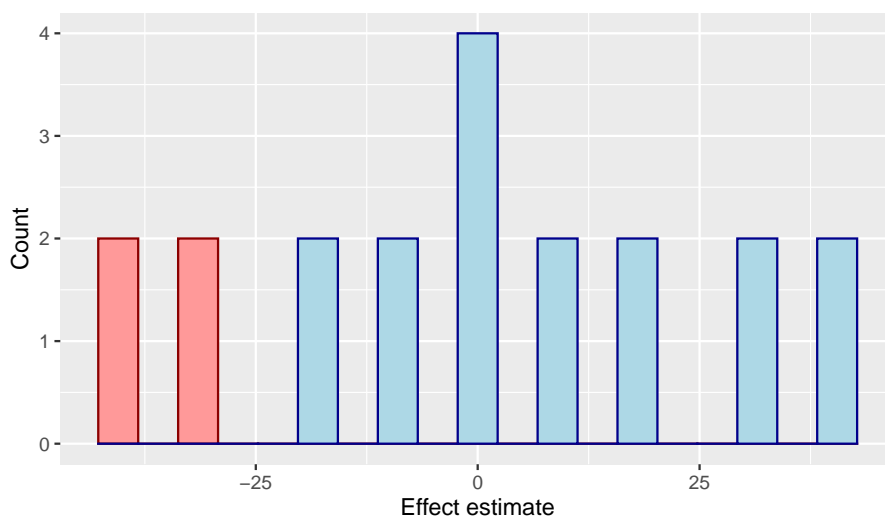
Appendix B: Randomization distribution of offspring alleles

The distribution of offspring haplotypes is often approximated by a first order hidden Markov model (HMM) (Haldane, 1919; Thompson, 2000; Bates et al., 2020). This model assumes “no interference”,

TABLE 6
Imputed data from a counterfactual experiment under the exact null hypothesis

i	\tilde{Z}_i	D_i	$D_i(1)$	$D_i(0)$	Y_i	$Y_i(1)$	$Y_i(0)$
1	1	1	1	?	120	120	120
2	0	1	1	?	120	120	120
3	0	0	0	?	75	75	75
4	1	0	?	1	165	165	165
5	1	0	?	0	135	135	135
6	0	0	?	0	105	105	105

Fig 7: Histogram of outcome differences for the exact null hypothesis



such that the location of crossover events are independent and the likelihood of an offspring inheriting a SNP from a given maternal or paternal haplotype depends only on the inheritance at adjacent loci. This induces a Poisson renewal process for the distribution of distances between crossovers, however, it should be noted that there is evidence of positive crossover interference in human meioses which results in a more even spread of crossovers than would be expected with random placement. Recent literature has therefore suggested that a Gamma renewal process may be a more appropriate model, although we do not provide this extension here (Otto and Payseur, 2019).

The randomness in our randomization distribution arises from both the location of crossover events (i.e. the transition distribution) and the small probability of independent de novo mutations (i.e. the emission distribution). Without loss of generality, we describe the distribution of offspring alleles inherited from the mother Z^m given maternal haplotypes M^m and M^f . Inheritance from the father is an independent instance of the same model. The transition distribution for the meiosis indicator at site j is assumed to be Poisson with mean equal to the genetic distance in centimorgans r_j between site $j - 1$ and j :

$$\begin{aligned} \mathbb{P}(U_j^m = u_{j-1}^m | U_{j-1}^m = u_{j-1}^m) &= \mathbb{P}(\text{even number of recombinations between } j - 1 \text{ and } j) \\ &= \frac{1}{2}(1 + e^{-2r_j}); \end{aligned}$$

$$\mathbb{P}(U_j^m = U_{j'}^m) = \frac{1}{2}(1 + e^{-2(d_j + \dots + d_{j'})})$$

where $u_{j-1}^m \in \{m, f\}$ and $j < j'$. Genetic distance is not proportional to physical distance on the chromosome due to the presence of recombination hotspots where crossover events are more likely to occur (Belmont et al., 2005; Bherer, Campbell and Auton, 2017). As r_j becomes large, the likelihood of an even number of recombinations approaches one half since genetically distant sites are transmitted almost independently.

The emission distribution is characterized by the probability of independent de novo single nucleotide mutations. A de novo mutation is said to occur when the base pair at some offspring SNP differs from the base pair they inherited from the parental haplotype. Within the context of the model, conditional on $U_j^m = u_j^m \in \{m, f\}$, each Z_j^m is sampled according to

$$\mathbb{P}(Z_j^m = M_j^{(u_j^m)} \mid U_j^m = u_j^m) = 1 - \epsilon \quad (15)$$

The probability of a de novo mutation ϵ is approximately $1 \cdot 10^{-8}$ in humans (Acuna-Hidalgo, Veltman and Hoischen, 2016).

The graphical structure of the hidden Markov model is shown in Figure 8. This graph differs from the more general structure shown in Figure 3b in that each meiosis indicator U_j^m depends only on the previous indicator U_{j-1}^m . Figure 9 embeds the hidden Markov model within the complete causal model used throughout Section 3.2.

Our primary use of the Markovian structure described above is to derive propensity scores for offspring haplotypes $Z_j^m \in \{0, 1\}$. In particular, our goal is to express the propensity score of some SNP Z_j^m given the adjustment set $(\mathbf{M}_j^{mf}, \mathbf{V}_B^m)$ of Theorem 1, where $\mathbf{V}_B^m = (\mathbf{M}_B^{mf}, \mathbf{Z}_B^m)$ and $\mathcal{B} \subseteq \mathcal{J} \setminus \{j\}$. Throughout this section we will assume that $\mathcal{B} = \{1, \dots, l\} \cup \{h, \dots, p\}$ for $l < j < h$. Suppressing conditioning on \mathbf{M}_j^{mf} and \mathbf{M}_B^{mf} for ease of notation, the propensity score for Z_j^m can be written as

$$\mathbb{P}(Z_j^m = 1 \mid \mathbf{Z}_B^m = \mathbf{z}_B^m) = \sum_{u \in \{m, f\}} \mathbb{P}(Z_j^m = 1 \mid U_j^m = u) \mathbb{P}(U_j^m = u \mid \mathbf{Z}_B^m = \mathbf{z}_B^m). \quad (16)$$

It is therefore more convenient to consider the conditional probability of U_j^m . We state the following theorem:

Theorem 3. *Using the conditional independence properties implied by Figure 3b, the conditional probability of $U_j^m = m$ can be factorized as*

$$\begin{aligned} & \mathbb{P}(U_j^m = m \mid \mathbf{Z}_B^m = \mathbf{z}_B^m) \\ & \propto \left[\sum_{u \in \{m, f\}} \beta_{h-1}^m(u) \mathbb{P}(U_{h-1}^m = u \mid U_j^m = m) \right] \left[\sum_{u \in \{m, f\}} \mathbb{P}(U_j^m = m \mid U_l^m = u) \alpha_l^m(u) \right]. \end{aligned}$$

The forward weights are defined recursively as

$$\begin{aligned} \alpha_1^m(u_1^m) &= \begin{cases} \frac{1}{2}(1 - \epsilon) & \text{if } M_1^{u_1^m} = z_1^m \\ \frac{1}{2}\epsilon & \text{if } M_1^{u_1^m} \neq z_1^m \end{cases} \\ \alpha_k^m(u_k^m) &= \sum_{u \in \{m, f\}} \mathbb{P}(Z_k^m = z_k^m \mid U_k^m = u_k^m) \mathbb{P}(U_k^m = u_k^m \mid U_{k-1}^m = u) \alpha_{k-1}^m(u), \quad k = 2, \dots, p \end{aligned}$$

and the backward weights are defined recursively as

$$\begin{aligned} \beta_p^m(u_p^m) &= 1 \\ \beta_k^m(u_k^m) &= \sum_{u \in \{m, f\}} \beta_{k+1}^m(u) \mathbb{P}(U_{k+1}^m = u \mid U_k^m = u_k^m) \mathbb{P}(Z_{k+1}^m = z_{k+1}^m \mid U_{k+1}^m = u), \quad k = 1, \dots, p-1, \end{aligned}$$

for $u_k^m \in \{m, f\}$ and $j, k \in \mathcal{J}$.

If we impose the simplifying assumption that $\epsilon = 0$, so that there is zero probability of de novo mutations, then the distribution of U_j^m derived in Theorem 3 can be simplified further.

Corollary 2. *Suppose the probability of a single nucleotide de novo mutation is $\epsilon = 0$ and suppose that the maternal haplotypes at $b_1, b_2 \in \mathcal{J}$ are heterozygous, where $b_1 < l < j < h < b_2$. That is, $M_{b_1}^m \neq M_{b_1}^f$ and $M_{b_2}^m \neq M_{b_2}^f$. Then the propensity score in Theorem 3 can equivalently be written as*

$$\begin{aligned} & \mathbb{P}(U_j^m = m \mid \mathbf{Z}_{\mathcal{B}}^m = \mathbf{z}_{\mathcal{B}}^m) \\ & \propto \left[\sum_{u \in \{m, f\}} \tilde{\beta}_{h-1}^m(u) \mathbb{P}(U_{h-1}^m = u \mid U_j^m = m) \right] \left[\sum_{u \in \{m, f\}} \mathbb{P}(U_j^m = m \mid U_l^m = u) \tilde{\alpha}_l^m(u) \right]. \end{aligned}$$

where

$$\begin{aligned} \tilde{\alpha}_{b_1+1}^m(u_{b_1+1}^m) &= \mathbb{P}(Z_{b_1+1}^m = z_{b_1+1}^m \mid U_{b_1+1}^m = u_{b_1+1}^m) \mathbb{P}(U_{b_1+1}^m = u_{b_1+1}^m \mid U_{b_1}^m = u_{b_1}^m) \\ \tilde{\alpha}_k^m(u_k^m) &= \sum_{u \in \{m, f\}} \mathbb{P}(Z_k^m = z_k^m \mid U_k^m = u_k^m) \mathbb{P}(U_k^m = u_k^m \mid U_{k-1}^m = u) \tilde{\alpha}_{k-1}^m(u), \quad k = b_1 + 2, \dots, p; \end{aligned}$$

and

$$\begin{aligned} \tilde{\beta}_{b_2-1}^m(u_{b_2-1}^m) &= \mathbb{P}(U_{b_2}^m = u_{b_2}^m \mid U_{b_2-1}^m = u_{b_2-1}^m) \mathbb{P}(Z_{b_2}^m = z_{b_2}^m \mid U_{b_2}^m = u_{b_2}^m) \\ \beta_k^m(u_k^m) &= \sum_{u \in \{m, f\}} \tilde{\beta}_{k+1}^m(u) \mathbb{P}(U_{k+1}^m = u \mid U_k^m = u_k^m) \mathbb{P}(Z_{k+1}^m = z_{k+1}^m \mid U_{k+1}^m = u), \quad k = 1, \dots, b_2 - 2. \end{aligned}$$

We will occasionally have multiple instruments lying in the same window. We will then need to compute a multivariate propensity score. We state the following corollary without proof because it follows almost immediately from Theorem 3.

Corollary 3. *Suppose we have a collection of instruments $\mathcal{J} = \{j_1, j_2, \dots, j_r\}$ such that $l < j_1 < j_2 < \dots < j_r < h$. Then the propensity score can be written as*

$$\mathbb{P}(U_{j_1}^m = u_{j_1}^m, U_{j_2}^m = u_{j_2}^m, \dots, U_{j_r}^m = u_{j_r}^m \mid \mathbf{Z}_{\mathcal{B}}^m = \mathbf{z}_{\mathcal{B}}^m) \quad (17)$$

$$= \mathbb{P}(U_{j_1}^m = u_{j_1}^m \mid \mathbf{Z}_{\mathcal{B}}^m = \mathbf{z}_{\mathcal{B}}^m) \prod_{k=2}^r \mathbb{P}(U_{j_k}^m = u_{j_k}^m \mid U_{j_{k-1}}^m = u_{j_{k-1}}^m, \mathbf{Z}_{\mathcal{B}}^m = \mathbf{z}_{\mathcal{B}}^m) \quad (18)$$

The first propensity score $\mathbb{P}(U_{j_1}^m = m \mid \mathbf{Z}_{\mathcal{B}}^m = \mathbf{z}_{\mathcal{B}}^m)$ takes the form in Theorem 3 and

$$\mathbb{P}(U_{j_k}^m = m \mid U_{j_{k-1}}^m = u_{j_{k-1}}^m, \mathbf{Z}_{\mathcal{B}}^m = \mathbf{z}_{\mathcal{B}}^m) \quad (19)$$

$$\propto \mathbb{P}(U_{j_k}^m = m \mid U_{j_{k-1}}^m = u_{j_{k-1}}^m) \left[\sum_{u \in \{m, f\}} \beta_{h-1}^m(u) \mathbb{P}(U_{h-1}^m = u \mid U_{j_k}^m = m) \right] \quad (20)$$

where $\beta_{h-1}^m(u)$ is the backward weight defined in Theorem 3.

Appendix C: Technical proofs

Proposition 1

Proof. From Assumption 1 we know that, conditional on $(M_j^m, M_j^f, F_j^m, F_j^f)$, Z_j^m and Z_j^f only depend on \mathbf{U}^m and \mathbf{U}^f , respectively, and exogenous mutation events. By (1), $Z_j = Z_j^m + Z_j^f$ given that $S = 1$ (fertilization occurs). Finally, by Assumption 2, the meiosis indicators \mathbf{U}^m and \mathbf{U}^f are independent of all confounders (A, C^m, C^f, C) . Therefore, the conditional independence statement immediately follows. \square

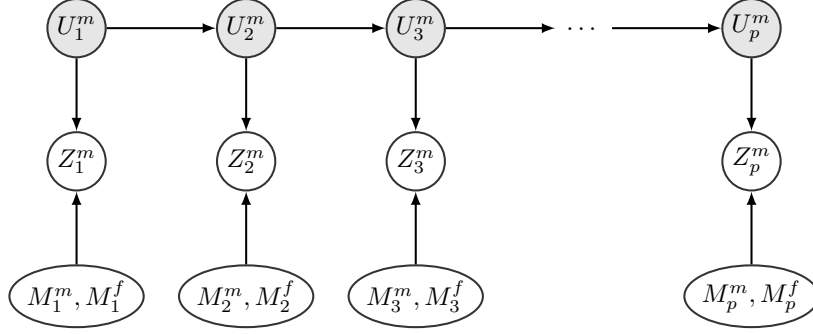


Fig 8: Graphical representation of Haldane's hidden Markov model.

Theorem 3

Proof. The conditional probability of U_j^m can be factorized as

$$\begin{aligned}
& \mathbb{P}(U_j^m = m \mid \mathbf{Z}_B^m = \mathbf{z}_B^m) \\
& \propto \mathbb{P}(U_j^m = m, \mathbf{Z}_B^m = \mathbf{z}_B^m) \\
& = \mathbb{P}(\mathbf{Z}_{h:p}^m = \mathbf{z}_{h:p}^m \mid U_j^m = m) \mathbb{P}(U_j^m = m, \mathbf{Z}_{1:l}^m = \mathbf{z}_{1:l}^m) \\
& = \left[\sum_{u \in \{m, f\}} \mathbb{P}(\mathbf{Z}_{(j+1):p}^m = \mathbf{z}_{(j+1):p}^m, U_{h-1}^m = u \mid U_j^m = m) \right] \\
& \quad \left[\sum_{u \in \{m, f\}} \mathbb{P}(U_j^m = m, U_l^m = u, \mathbf{Z}_{1:l}^m = \mathbf{z}_{1:l}^m) \right] \\
& = \left[\sum_{u \in \{m, f\}} \mathbb{P}(\mathbf{Z}_{(j+1):p}^m = \mathbf{z}_{(j+1):p}^m \mid U_{h-1}^m = u) \mathbb{P}(U_{h-1}^m = u \mid U_j^m = m) \right] \\
& \quad \left[\sum_{u \in \{m, f\}} \mathbb{P}(U_j^m = m \mid U_l^m = u) \mathbb{P}(U_l^m = u, \mathbf{Z}_{1:l}^m = \mathbf{z}_{1:l}^m) \right] \\
& = \left[\sum_{u \in \{m, f\}} \beta_{h-1}^m(u) \mathbb{P}(U_{h-1}^m = u \mid U_j^m = m) \right] \left[\sum_{u \in \{m, f\}} \mathbb{P}(U_j^m = m \mid U_l^m = u) \alpha_l^m(u) \right].
\end{aligned}$$

The forward weight $\alpha_1^m(u_1^m)$ for some $u_1^m \in \{m, f\}$ can be derived as

$$\begin{aligned}
\alpha_1^m(u_1^m) & = \mathbb{P}(U_1^m = u_1^m, Z_1^m = z_1^m) \\
& = \mathbb{P}(Z_1^m = z_1^m \mid U_1^m = u_1^m) \mathbb{P}(U_1^m = u_1^m) \\
& = \frac{1}{2} \mathbb{P}(Z_1^m = z_1^m \mid U_1^m = u_1^m)
\end{aligned}$$

where the emission probability is known. A recursive expression for the forward weight $\alpha_j^m(u_j^m)$ for

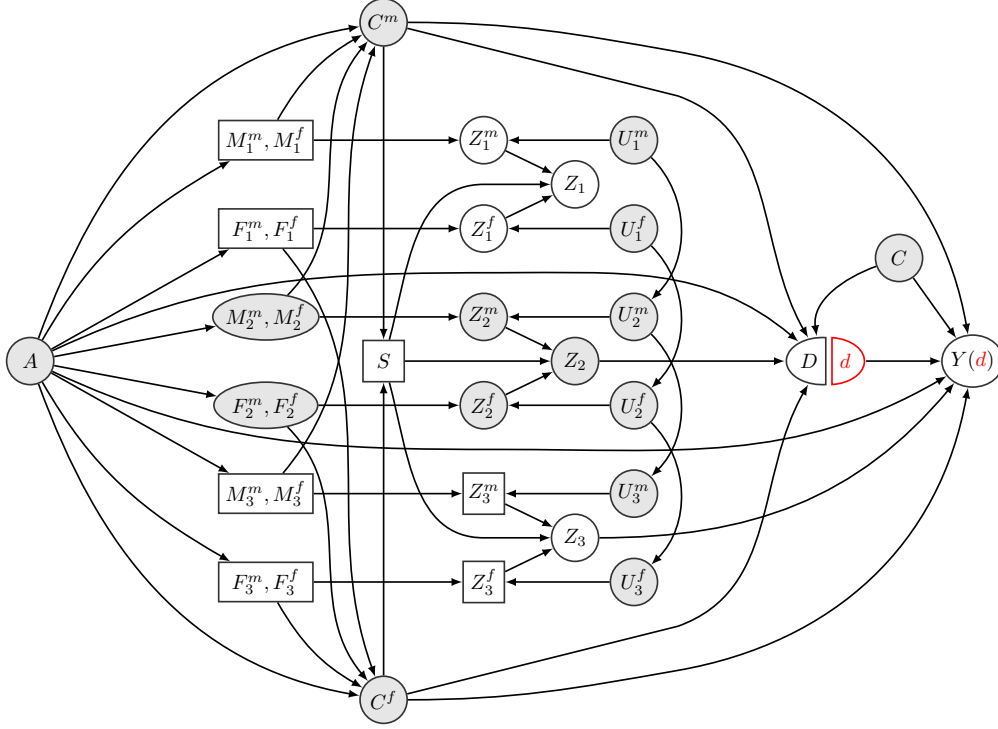


Fig 9: Haldane's hidden Markov model embedded in the working example in Figure 2.

$j = 2, \dots, p$ can be derived as

$$\begin{aligned}
 \alpha_j^m(u_j^m) &= \mathbb{P}(U_j^m = u_j^m, \mathbf{Z}_{1:j}^m = \mathbf{z}_{1:j}^m) \\
 &= \sum_{u \in \{m, f\}} \mathbb{P}(U_j^m = u_j^m, U_{j-1}^m = u_{j-1}^m, \mathbf{Z}_{1:j}^m = \mathbf{z}_{1:j}^m) \\
 &= \sum_{u \in \{m, f\}} \mathbb{P}(Z_j^m = z_j^m \mid U_j^m = u_j^m) \mathbb{P}(U_j^m = u_j^m \mid U_{j-1}^m = u) \mathbb{P}(U_{j-1}^m = u, \mathbf{Z}_{1:(j-1)}^m = \mathbf{z}_{1:(j-1)}^m) \\
 &= \sum_{u \in \{m, f\}} \mathbb{P}(Z_j^m = z_j^m \mid U_j^m = u_j^m) \mathbb{P}(U_j^m = u_j^m \mid U_{j-1}^m = u) \alpha_{j-1}^m(u).
 \end{aligned}$$

The backward weight $\beta_j^m(u_j^m)$ for some $u_j^m \in \{m, f\}$ and $j = 1, \dots, p-1$ can be derived as

$$\begin{aligned}
 \beta_j^m(u_j^m) &= \mathbb{P}(\mathbf{Z}_{(j+1):p}^m = \mathbf{z}_{(j+1):p}^m \mid U_j^m = u_j^m) \\
 &= \sum_{u \in \{m, f\}} \mathbb{P}(\mathbf{Z}_{(j+1):p}^m = \mathbf{z}_{(j+1):p}^m, U_{j+1}^m = u \mid U_j^m = u_j^m) \\
 &= \sum_{u \in \{m, f\}} \mathbb{P}(\mathbf{Z}_{(j+2):p}^m = \mathbf{z}_{(j+2):p}^m \mid U_{j+1}^m = u) \mathbb{P}(Z_{j+1}^m = z_{j+1}^m \mid U_{j+1}^m = u) \mathbb{P}(U_{j+1}^m = u \mid U_j^m = u_j^m).
 \end{aligned}$$

Writing the probability of U_p^m shows that $\beta_p^m(u) = 1$ for all $u \in \{m, f\}$. \square

Corollary 2

Proof. The proof involves some manipulation of conditional independencies. We simplify the probability with respect to b_1 and omit simplification with respect to b_2 for brevity. As with the proof of

Theorem 3 we begin by factorising the conditional probability of U_j^m .

$$\mathbb{P}(U_j^m = m \mid \mathbf{Z}_{\mathcal{B}}^m = \mathbf{z}_{\mathcal{B}}^m) = \frac{\mathbb{P}(\mathbf{Z}_{h:p}^m = \mathbf{z}_{h:p}^m \mid U_j^m = m)\mathbb{P}(U_j^m = m, \mathbf{Z}_{1:l}^m = \mathbf{z}_{1:l}^m)}{\mathbb{P}(\mathbf{Z}_{\mathcal{B}}^m = \mathbf{z}_{\mathcal{B}}^m)}. \quad (21)$$

Since $b_1 < j$ we are concerned with simplifying the second probability in the numerator of equation (21).

$$\begin{aligned} & \mathbb{P}(U_j^m = m, \mathbf{Z}_{1:l}^m = \mathbf{z}_{1:l}^m) \\ &= \sum_{u \in \{m, f\}} \mathbb{P}(U_j^m = m, U_{b_1}^m = u, \mathbf{Z}_{1:l}^m = \mathbf{z}_{1:l}^m) \\ &= \sum_{u \in \{m, f\}} \mathbb{P}(U_j^m = m, \mathbf{Z}_{(b_1+1):l}^m = \mathbf{z}_{(b_1+1):l}^m \mid U_{b_1}^m = u)\mathbb{P}(U_{b_1}^m = u, \mathbf{Z}_{1:b_1}^m = \mathbf{z}_{1:b_1}^m) \\ &= \mathbb{P}(U_j^m = m, \mathbf{Z}_{(b_1+1):l}^m = \mathbf{z}_{(b_1+1):l}^m \mid U_{b_1}^m = m)\mathbb{P}(U_{b_1}^m = m, \mathbf{Z}_{1:b_1}^m = \mathbf{z}_{1:b_1}^m) \\ &= \mathbb{P}(U_{b_1}^m = m, \mathbf{Z}_{1:b_1}^m = \mathbf{z}_{1:b_1}^m) \sum_{u \in \{m, f\}} \mathbb{P}(U_j^m = m \mid U_{j-1}^m = u)\mathbb{P}(U_{j-1}^m = u, \mathbf{Z}_{(b_1+1):(j-1)}^m = \\ & \quad \mathbf{z}_{(b_1+1):(j-1)}^m \mid U_{b_1}^m = m) \\ &= \mathbb{P}(U_{b_1}^m = m, \mathbf{Z}_{1:b_1}^m = \mathbf{z}_{1:b_1}^m) \sum_{u \in \{m, f\}} \mathbb{P}(U_j^m = m \mid U_{j-1}^m = u)\tilde{\alpha}_{j-1}^m(u). \end{aligned}$$

where

$$\begin{aligned} \tilde{\alpha}_{b_1+1}^m(u_{b_1+1}^m) &= \mathbb{P}(\mathbf{Z}_{b_1+1}^m = \mathbf{z}_{b_1+1}^m \mid U_{b_1+1}^m = u_{b_1+1}^m)\mathbb{P}(U_{b_1+1}^m = u_{b_1+1}^m \mid U_{b_1}^m = m) \\ \tilde{\alpha}_k^m(u_k^m) &= \sum_{u \in \{m, f\}} \mathbb{P}(\mathbf{Z}_k^m = \mathbf{z}_k^m \mid U_k^m = u_k^m)\mathbb{P}(U_k^m = u_k^m \mid U_{k-1}^m = u)\tilde{\alpha}_{k-1}^m(u), \\ & \text{for } k = b_1 + 2, \dots, j - 1. \end{aligned}$$

We now factorize the denominator of equation (21).

$$\mathbb{P}(\mathbf{Z}_{\mathcal{B}}^m = \mathbf{z}_{\mathcal{B}}^m) = \mathbb{P}(\mathbf{Z}_{(b_1+1):l}^m = \mathbf{z}_{(b_1+1):l}^m, \mathbf{Z}_{h:p}^m = \mathbf{z}_{h:p}^m \mid U_{b_1}^m = m)\mathbb{P}(U_{b_1}^m = m, \mathbf{Z}_{1:b_1}^m = \mathbf{z}_{1:b_1}^m).$$

Substituting these simplified expressions back in equation (21) we obtain

$$\begin{aligned} & \mathbb{P}(U_j^m = m \mid \mathbf{Z}_{\mathcal{B}}^m = \mathbf{z}_{\mathcal{B}}^m) \\ &= \frac{\mathbb{P}(\mathbf{Z}_{h:p}^m = \mathbf{z}_{h:p}^m \mid U_j^m = m)\mathbb{P}(U_{b_1}^m = m, \mathbf{Z}_{1:b_1}^m = \mathbf{z}_{1:b_1}^m) \sum_{u \in \{m, f\}} \mathbb{P}(U_j^m = m \mid U_{j-1}^m = u)\tilde{\alpha}_{j-1}^m(u)}{\mathbb{P}(\mathbf{Z}_{(b_1+1):l}^m = \mathbf{z}_{(b_1+1):l}^m, \mathbf{Z}_{h:p}^m = \mathbf{z}_{h:p}^m \mid U_{b_1}^m = m)\mathbb{P}(U_{b_1}^m = m, \mathbf{Z}_{1:b_1}^m = \mathbf{z}_{1:b_1}^m)} \\ &= \frac{\mathbb{P}(\mathbf{Z}_{h:p}^m = \mathbf{z}_{h:p}^m \mid U_j^m = m) \sum_{u \in \{m, f\}} \mathbb{P}(U_j^m = m \mid U_{j-1}^m = u)\tilde{\alpha}_{j-1}^m(u)}{\mathbb{P}(\mathbf{Z}_{(b_1+1):l}^m = \mathbf{z}_{(b_1+1):l}^m, \mathbf{Z}_{h:p}^m = \mathbf{z}_{h:p}^m \mid U_{b_1}^m = m)}. \end{aligned} \quad (22)$$

which does not depend on $\mathbf{Z}_{1:k}^m$. \square

Appendix D: Simulation

D.1. Further description of the simulation setting

Table 7: Description of the simulation variables and parameters

Variable	Description of how the variable is constructed	Parameters
$M_i^m, M_i^f, F_i^m, F_i^f$	The parental haplotypes are constructed to allow linkage disequilibrium in nearby SNPs. For each parental haplotype we first sample from a p -variate normal such that $X_{ij} \sim \mathcal{N}(0, 1)$ and $Cov(X_{ij}, X_{ik}) = \rho^{ j-k }$, $0 < \rho < 1$, $j, k \in \mathcal{J}$. Thresholds $V_{ij} \sim Unif(a, b)$ are sampled and the haplotypes are defined as $M_{ij}^m = I\{X_{ij} > V_{ij}\}$ where $I\{\cdot\}$ is the indicator function (and similarly for the other haplotypes).	$\rho = 0.75$ $a = \Phi^{-1}(0.6)$ $b = \Phi^{-1}(0.95)$ where $\Phi^{-1}(\cdot)$ is the inverse normal CDF.
C_i^m, C_i^f	We first define a variable $\hat{\mu}_i^m = \frac{1}{p} \sum_{j=1}^p (M_{ij}^m + M_{ij}^f).$ It follows from our construction of the parental haplotypes that $\mu^m = E[\hat{\mu}^m] = 2 \left(1 - \frac{1}{b-a} \int_a^b \Phi(x) dx \right).$ where $\Phi(\cdot)$ is the normal CDF. For each individual i we sample the parental confounder such that $C_i^m \sim \mathcal{N}(\hat{\mu}_i^m - \mu^m, 1).$ We follow an identical procedure for C_i^f .	N/A
C_i	We construct the offspring confounder as $C_i \sim \mathcal{N}(0, 1).$	N/A

$\mathbf{Z}_i^m, \mathbf{Z}_i^f$	<p>We sample the offspring haplotypes using Algorithm 1 in Bates et al. (2020). This algorithm unconditionally samples a full haplotype \mathbf{Z}_i^m or \mathbf{Z}_i^f according to the hidden Markov model described in Appendix B. It depends on the genetic distances \mathbf{r} and de novo mutation rate ϵ. We sample $r_j \sim Unif(c, d)$ and set $r_k = \infty$ for $k = 37, 62, 86, 112$ so that the instruments are unconditionally independent. From these haplotypes we choose a subset $\mathcal{J}_g \subset \mathcal{J}$ to be instruments.</p>	$\epsilon = 10^{-8}$ $c = 0$ $d = 0.75$ $\mathcal{J}_g = \{25, 50, 75, 100, 125\}$
D_i	<p>The exposure follows a linear structural equation model</p> $D_i = \gamma^\top \mathbf{Z}_i + \theta^m C_i^m + \theta^f C_i^f + \theta^c C_i + \nu_i$ <p>where $\nu_i \sim \mathcal{N}(0, 0.7)$. We choose γ so that it is zero everywhere except for $\gamma_{24}, \gamma_{49}, \gamma_{74}, \gamma_{99}$ and γ_{124} which represent causal variants. The parameters are chosen so that $Var(D_i) = 1$.</p>	$\theta^m = \theta^f = \sqrt{0.3}$ $\theta^c = \sqrt{0.75}$ $\gamma_j = \sqrt{0.1}$ for $j = 24, 49, 74, 99, 124$.
Y_i	<p>The outcome follows a linear structural equation model</p> $Y_i = \beta D_i + \delta^\top \mathbf{Z}_i + \phi^m C_i^m + \phi^f C_i^f + \phi^c C_i + \nu_i$ <p>where $\nu_i \sim \mathcal{N}(0, 0.7)$. We choose δ so that it is zero everywhere except for $\delta_{23}, \delta_{27}, \delta_{48}, \delta_{52}, \delta_{73}, \delta_{77}, \delta_{98}, \delta_{102}, \delta_{123}$ and δ_{127} which represent pleiotropic variants. The parameters are chosen so that $Var(Y_i) = 1$.</p>	$\beta = 0$ $\phi^m = \phi^f = \sqrt{0.3}$ $\phi^c = \sqrt{0.75}$ $\delta_j = \sqrt{0.05}$ for $j = 23, 27, 48, 52, 73, 77, 98, 102, 123, 127$.

Theorem 1 implies that a sufficient adjustment set for this simulation is

$$(\mathbf{M}_{\mathcal{B}_g}^{mf}, \mathbf{F}_{\mathcal{B}_g}^{mf}, \mathbf{Z}_{\mathcal{B}}) \quad (23)$$

where

$$\mathcal{B} = \mathcal{J} \setminus \{24, 25, 26, 49, 50, 51, 99, 74, 75, 76, 99, 100, 101, 124, 125, 126\}$$

and

$$\mathcal{B}_g = \mathcal{B} \cup \{25, 50, 75, 100, 125\}.$$

D.2. An illustration of the simulation setup

To make our setup more tangible, [Table 8](#) shows the first 6 lines of observed and counterfactual data (in red) from the simulation for one of the instruments and corresponding parental haplotypes. We can see that individual 4 will provide almost no information for a test of the null hypothesis;

both of her parents are homozygous so there is no randomization in her genotype outside of de novo mutations. Conversely, both of individual 1's parents are heterozygous so she could receive both major alleles, both minor alleles or one of each.

Suppose we wish to test the null hypothesis $H_0 : \beta = -0.3$. Column \tilde{Z}_i in Table 8 shows a counterfactual draw of each individual's instrument conditional on the adjustment set given in Equation (23) in Appendix D, along with the adjusted outcome $Q_i(-0.3)$. Note that \tilde{Z}_i is independent of $Q_i(-0.3)$ by construction, so the null hypothesis is necessarily satisfied for this counterfactual. As expected individual 4 has the same genotype in this counterfactual, however, individual 1 inherits both minor alleles in this case. Figure 10 plots a distribution of 10,000 counterfactual test statistics drawn under the null hypothesis. The test statistic is the F-statistic from a regression of the adjusted outcome on the instruments. The bars highlighted in red are larger than the observed test statistic, such that the almost exact p-value is around 0.13.

TABLE 8
First 6 rows of observed data from the simulation

i	Z_i	\tilde{Z}_i	M_i^m	M_i^f	F_i^m	F_i^f	D_i	Y_i	$Q_i(-0.3)$
1	1	2	1	0	1	0	1.11	0.73	1.06
2	0	1	1	0	0	0	0.83	-0.52	0.77
3	1	1	1	0	0	0	0.94	0.31	0.59
4	0	0	0	0	0	0	1.43	3.30	3.73
5	0	0	0	0	0	0	0.15	1.34	1.38
6	0	0	0	0	0	0	-0.14	1.60	1.56

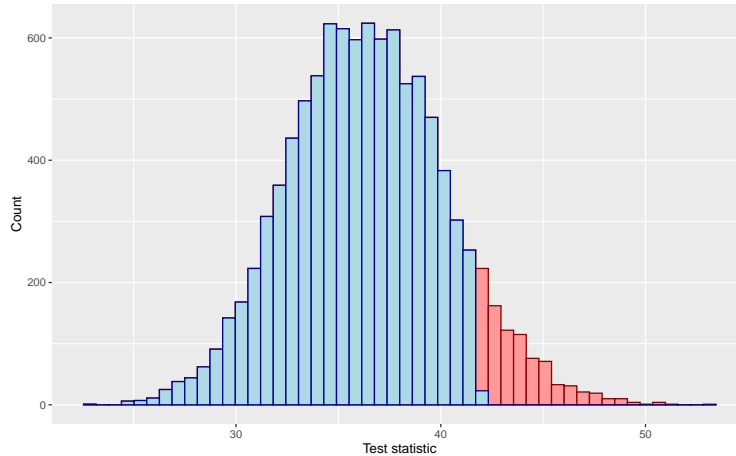


Fig 10: Histogram of 10,000 test statistics under the null hypothesis $H_0 : \beta = -0.3$